Chapter 3 Results

3.1 Accurate pK_a computation

Single molecule studies to compute pK_a values, PA values (for a definition of PA values see: eq. 2.10) and the electrostatic solvation free energies were performed for a heterogeneous set of organic compounds (see Figure 3.1a and 3.1b) Computed energetics of gas phase protonation based on quantum mechanical density functional theory (DFT) using the Becke-half&half (Becke($^1/_2$))[75] and B3LYP[76, 77] functionals on optimized molecular geometries converged sufficiently well with experimental data (see chapter 3.1.2). The electrostatic contribution to the solvation energies of protonated and deprotonated compounds were calculated by solving the Poisson equation using atomic charges generated by fitting the electrostatic potential derived from the molecular wave functions in vacuum. This method is referred as the *two-step* procedure and was coherently explained in chapter 2.7. The combination of gas phase and electrostatic solvation free energies by means of the thermodynamic cycle enabled us to compute pK_a values for a variety of compounds, which cover six distinct chemical groups (carboxylic acids, benzoic acids, phenols, imides, pyridines and imidazoles). The acid-base equilibria of 26 of the 29 titratable substances, which are depicted in Figure 3.1a and 3.1b, will be discussed first, separately from p-, m- and o-methyl phenol. Estimation of pK_a values for three methylated phenols are discussed in a subsequent chapter, because an extended protocol to generate partial atomic charges was applied and compared with the standard protocol described in chapter 2.6 and 2.8.

3.1.1 pK_a values for a heterogeneous group of organic molecules

Within the framework set by the thermodynamic cycle shown in Scheme 2.1 the present study evaluated pK_a values for a spectrum of titratable compounds, which are depicted in Figure 3.1a and 3.1b. The considered substances possess either a titratable oxygen (carboxylic acids benzoic acids and phenols (see Figure 3.1a) or a titratable nitrogen (imidazoles, pyridines, imides. The computed pK_a values for 26 compounds obtained with the Becke($^1/_2$)[75] and B3LYP[76, 77] functional are accurate with an RMS deviation of 0.53 and 0.57 pK_a units and a maximum error of 1.0 and 1.3 pK_a units, respectively (see Table 3.1 and Figure 3.2a,b and 3.3a,b).[41] All electronic energies were computed using the cc-pVQZ basis set[79, 80] either with Becke($^1/_2$) or with B3LYP. Solvation energies were computed with the *two-step* procedure (see section 2.7). Electrostatic solvation free energies were obtained from a balanced combination of an QC ESP[109] obtained with the DFT functional Becke($^1/_2$) or B3LYP with the 6-31G** basis set and a set of vdW radii, which was given in section 2.7. The RESP[69, 70] procedure was used throughout the present thesis to transform the QC ESP into point charges (see chapter 2.3 and 2.7). Solvation energies were computed using a solute dielectric constant equal to one in vacuum and in the condensed phase. All computed pK_a values based on Becke($^1/_2$) emloyed a $\Delta G_{solv}(H^+) = -261.94$ kcal/mol, whereas computed pK_a obtained with B3LYP values employed a $\Delta G_{solv}(H^+) = -265.74$ kcal/mol (see chapter 2.5 and 2.7).

Figure 3.1a: Compounds with a titratable an O-Atom, whose pK_a values, PA values and electrostatic solvation free energies were studied.

carboxylic acids

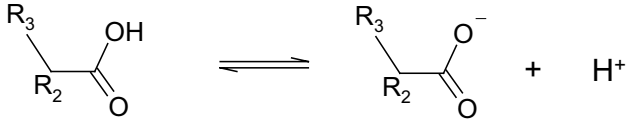

propionic acid:	R_2: CH_2	R_3: CH_3
butyric acid:	R_2: CH_2	**R_3: C_2H_5**
2-chloropropionic acid:	**R_2: CClH**	R_3: CH_3
3-chloropropionic acid:	R_2: CH_2	**R_3: $CClH_2$**

benzoic acids

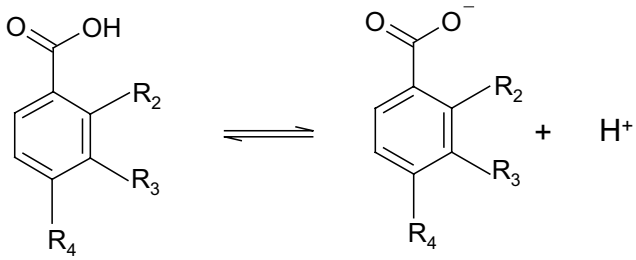

benzoic acid:	R_2: H	R_3: H	R_4: H
3-methyl-benzoic acid:	R_2: H	**R_3: CH3**	R_4: H
4-methyl-benzoic acid:	R_2: H	R_3: H	**R_4: CH3**
4-chloro-benzoic acid:	R_2: H	R_3: H	**R_4: Cl**

phenols

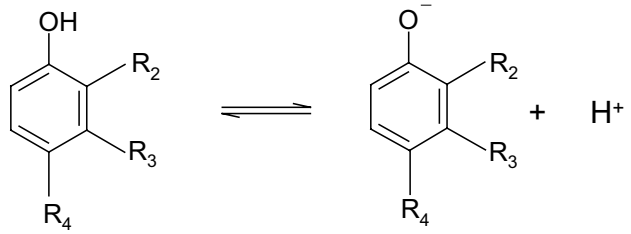

phenol	R_2: H	R_3: H	R_4: H
2-methyl-phenol:	**R_2: CH_3**	R_3: H	R_4: H
2-amino-phenol:	**R_2: NH_2**	R_3: H	R_4: H
3-methyl-phenol:	R_2: H	**R_3: CH3**	R_4: H
3-amino-phenol:	R_2: H	**R_3: NH_2**	R_4: H
3-chloro-phenol:	R_2: H	**R_3: Cl**	R_4: H
4-methyl-phenol:	R_2: H	R_3: H	**R_4: CH_3**
4-amino-phenol:	R_2: H	R_3: H	**R_4: NH_2**
4-chloro-phenol:	R_2: H	R_3: H	**R_4: Cl**

Figure 3.1b: Compounds with a titratable a N-Atom, whose pK_a values, PA values and electrostatic solvation free energies were studied.

imides:

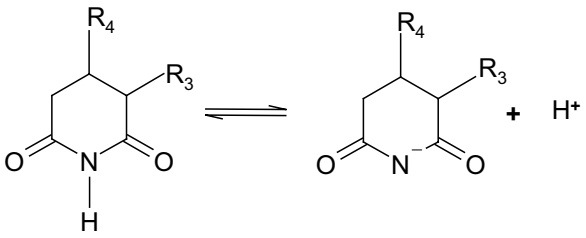

glutaconimide: R_3: H R_4: H

glutarimide: R_3: 2H R_4: 2H

pyridines:

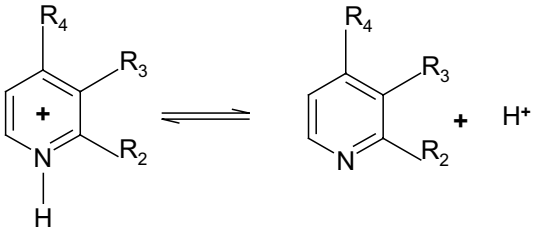

pyridine:	R_2: H	R_3: H	R_4: H
2-methyl-pyridine:	**R_2: CH_3**	R_3: H	R_4: H
2-amino-pyridine:	**R_2: NH_2**	R_3: H	R_4: H
3-chloro-pyridine:	R_2: H	**R_3: Cl**	R_4: H
2-methyl-pyridine:	R_2: H	R_3: H	**R_2: CH_3**
2-amino-pyridine :	R_2: H	R_3: H	**R_2: NH_2**

imidazoles:

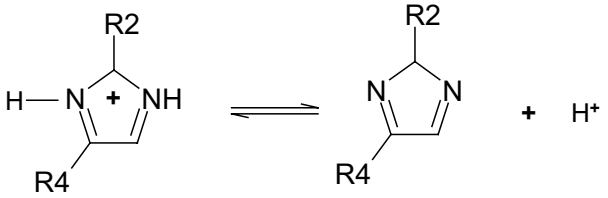

imidazole:	R_2: H	R_4: H
2-methyl-imidazole:	**R_2: CH_3**	R_4: H
2-amino-imidazole:	**R_2: NH_2**	R_4: H
2-chloro-imidazole:	**R_2: Cl**	R_4: H
4-chloro-imidazole:	R_2: H	**R_4: CH3**

Inspection of the correlation diagrams (see Figure 3.2a and 3.3a) reveals that the computed absolute pK_a values of all six functional groups scatter around the diagonal without a systematic deviation. This is the case for the results based on PA values obtained with Becke($^1/_2$) (Figure 3.2a) as well as for B3LYP (Figure 3.3a). Figure 3.2b and 3.3b also illustrate the accuracy of the applied method for six compounds, which represent the six functional groups shown in Figure 3.1a and 3.1b. Computed pK_a values in Figure 3.2b based on Becke($^1/_2$)/cc-pVQZ for phenol and pyridine match exactly the measured values, whereas the other four compounds exhibit a deviation that is accidentally rather than systematic. B3LYP leads to deviations for five of the six computed pK_a values (see Figure 3.3b). Here, only the absolute pK_a value of phenol matches the experimental result.

Carboxylic and benzoic acids. Regarding the protonation behavior it makes sense to consider the carboxylic and benzoic acids together, since they possess the same titratable group. Four carboxylic acids and four benzoic acids were included in the present study. I chose the considered substitutents to investigate the influence of aliphatic groups and chlorine on the acidity of the COOH group. The pK_a and PA of all benzoic acids (see Table 3.1 and 3.2) were calculated with the carboxyl oxygens in the benzene ring plane. The out-of-plane conformation of benzoic acid in the gas phase is clearly disfavored in the neutral and anionic charge state. Employing this conformation would lower the computed pK_a values by −2.5 units. Calculation of electronic energies E_0(AH) for m-substituted benzoic acids were performed with the OH-group of the protonated species pointing away from the methyl group.

Becke($^1/_2$)[75] reproduces the absolute pK_a values of the eight compounds accurately (see Table 3.1). The largest deviations between measured and computed pK_a values occur for propionic acid and benzoic acid with 0.87 pK_a units and 0.96 pK_a units, respectively. The influence of a chlorine atom on the protonation behavior is reproduced accurately in terms of absolute and relative pK_a values (see Table 3.1). The influence of a CH_3 or CH_2 substituent on the acid-base equilibrium is covered in terms of absolute pK_a values but not in terms of relative pK_a values as Table 3.1 reveals. Identical pK_a values were measured for propionic acid and butyric acid, which differ only by one additional CH_2 group. Albeit computed absolute pK_a values deviate by less than one pK_a unit from its measured counterparts, the influence of an additional methylene group on the acidity of the COOH group is exaggerated considerably as the computed pK_a value of butyric acid reveals (see Table 3.1).

B3LYP [76, 77] reproduces measured pK_a values for substituted benzoic acids equally well as Becke($^1/_2$), but has difficulties to cover measured pK_a values of carboxylic acids. Computed pK_a values for propionic acid and 2-chloropropionic acid deviate from the experimental results by more than one pK_a unit. As it is the case for the results obtained with Becke($^1/_2$) the influence of a CH_3 or CH_2 substituent on the acidity of the COOH group is overestimated.

Phenols: Substituted phenols were included in the present study. The geometries used for the calculation of PA, ΔG_{solv} and pK_a correspond to the lowest energy conformations in the gas phase. For the substituted phenols depicted in Figure 3.1a the lowest energy of the protonated forms is generally achieved with titratable proton pointing away from the substitutent. The RMS deviation of the pK_a values for this group is 0.54 when calculated with Becke($^1/_2$)[75] and 0.34 when the B3LYP[76, 77] method is applied. The largest deviations using Becke($^1/_2$) were found for o-amino-phenol and m-chlorophenol, with 1.00 and 0.83 pK_a units, respectively, while with B3LYP the largest deviation is only 0.62 pK_a units for o-aminophenol.

Table 3.1. Calculated and measured pK_a values for the 26 considered compounds, which are discussed in chapter 3.1.1 and illustrated in Figure 3.1a and 3.1b. The computational details to derive absolute pK_a values were given in chapter 3.1.1 and 2.8.

substances	formula	Becke($^1/_2$)	B3LYP	measured
carboxylic acids				
propionic acid	C_2H_5-COOH/COO^-	3.98	3.52	4.85[a]
butyric acid	C_3H_7-COOH/COO^-	5.02	4.93	4.85[a]
α-chloropropionic acid	Cl-C_2H_4-COOH/COO^-	3.07	2.70	2.85[a]
β-chloropropionic acid	Cl-C_2H_4-COOH/COO^-	3.45	2.89	4.10[a]
benzoic acids				
benzoic acid	PhCOOH/$PhCOO^-$	3.26	3.49	4.22[a]
p-methylbenzoic acid	4-CH_3-PhCOOH/$PhCOO^-$	4.91	4.25	4.37[a]
m-methylbenzoic acid	3-CH_3-PhCOOH/$PhCOO^-$	4.10	3.51	4.22[a]
p-chlorobenzoic acid	4-Cl-PhCOOH/$PhCOO^-$	3.12	3.69	3.98[a]
phenols				
phenol	PhOH/PhO^-	9.99	9.95	9.98[b]
m-aminophenol	3-NH_2-PhOH/PhO^-	10.18	10.25	9.87[b]
o-aminophenol	2-NH_2-PhOH/PhO^-	10.64	10.39	9.78[c]
m-chlorophenol	3-Cl-PhOH/PhO^-	9.72	9.25	9.02[b]
o-chlorophenol	2-Cl-PhOH/PhO^-	8.89	8.72	8.56[b]
imides				
glutarimide	C_5H_4ONHO/ON^-O	12.29	11.58	11.75[c]
glutaconimide	C_5H_6ONHO/ON^-O	10.13	10.23	9.83[c]
pyridines				
pyridine	$C_5H_5NH^+/C_5H_5N$	5.26	5.82	5.25[d]
2-methylpyridine	2-CH_3-$C_5H_5NH^+/C_5H_5N$	5.33	5.67	5.68[d]
4-methylpyridine	4-CH_3-$C_5H_5NH^+/C_5H_5N$	5.59	5.84	6.02[d]
3-chloropyridine	3-Cl-$C_5H_5NH^+/C_5H_5N$	2.92	3.66	2.84[d]
2-aminopyridine	2-NH_2-$C_5H_5NH^+/C_5H_5N$	6.27	6.57	6.82[d]
4-aminopyridine	4-NH_2-$C_5H_5NH^+/C_5H_5N$	9.47	10.01	9.11[d]
imidazoles				
imidazole	$C_3H_3N_2H_2^+/N_2H$	7.82	7.98	7.00[e]
2-methylimidazole	2-CH_3-$C_3H_3N_2H_2^+/N_2H$	7.69	8.18	7.80[e]
4-methylimidazole	4-CH_3-$C_3H3N_2H_2^+/N_2H$	7.44	7.34	7.45[f]
2-aminoimidazole	2-NH_2.$C_3H3N_2H_2^+/N_2H$	8.98	8.79	8.50[e]
2-chloroimidazole	2-Cl-$C_3H3N_2H_2^+/N_2H$	2.73	3.03	3.55[e]

[a] Reference 3 [b] Reference 40 [c] Calculated using Advanced ChemistryDevelopment (ACD) Software Solaris V4.67 (1994–2003,ACD) [d] Reference 159 [e] Reference 164 [f] Reference 36

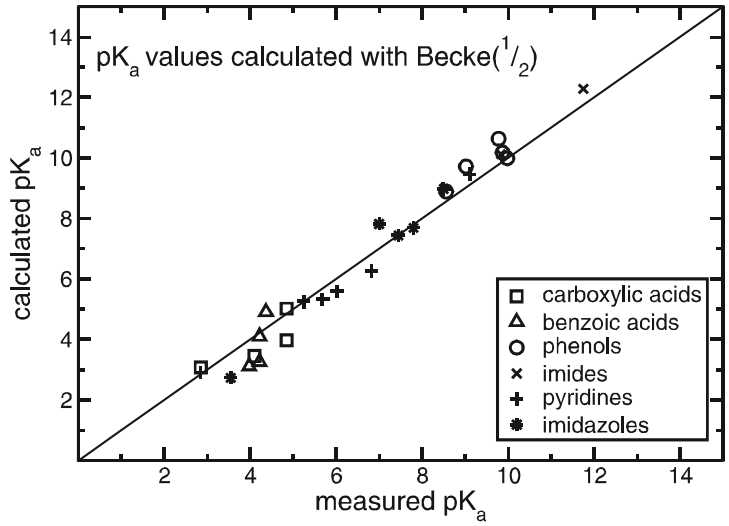

Figure 3.2a. Correlation diagram of experimental and calculated pK_a values for the 26 compounds listed in Table 3.1. The computed pK_a values are based on electronic energies E_0 obtained with Becke($^1/_2$)/cc-pVQZ. Atomic partial charges used for computation of solvation energies were calculated on optimized geometries with Becke($^1/_2$)/6-31G**. The pK_a values displayed in this Figure were calculated with a $\Delta G_{solv}(H^+)$ value of –261.94 kcal/mol yielding an RMS deviation of 0.53 pK_a units.

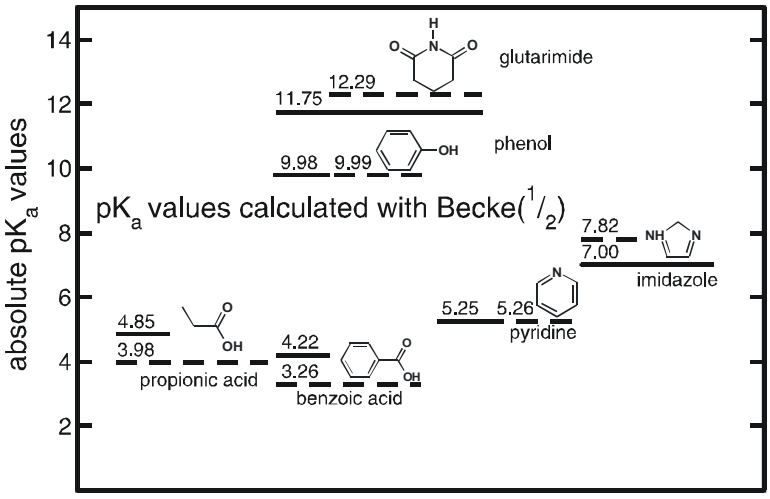

Figure 3.2b. Comparison of experimental (solid line) and calculated (dashed line) pK_a values for six compounds, which represent the six functional groups depicted in Figure 3.1a,b. The considered compounds are depicted in their neutral state. The computed pK_a values are based on electronic energies E_0 obtained with Becke($^1/_2$)/cc-pVQZ, atomic partial charges derived from a QC computation with Becke($^1/_2$)/6-31G** and a $\Delta G_{solv}(H^+)$ value of –261.94 kcal/mol.

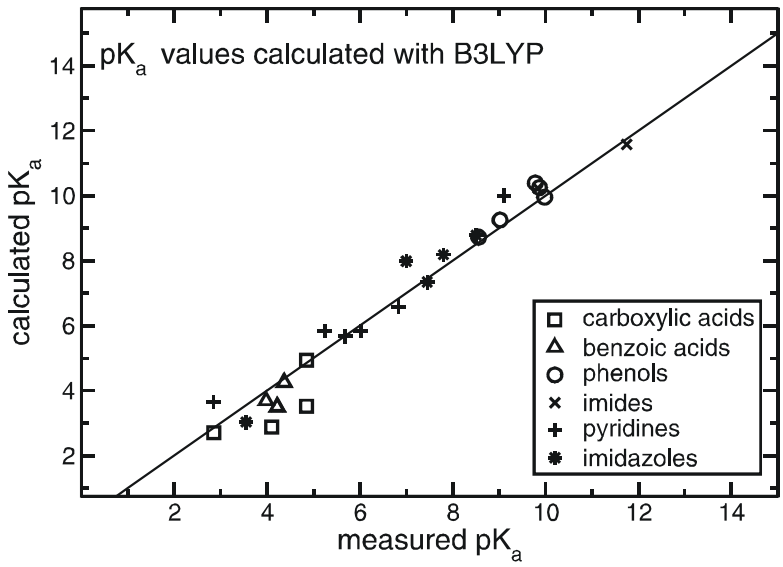

Figure 3.3a. Correlation diagram of experimental and calculated pK_a values for the 26 compounds listed in Table 3.1. The computed pK_a values are based on electronic energies E_0 obtained with B3LYP/cc-pVQZ. Atomic partial charges used for computation of solvation energies were calculated on optimized geometries with B3LYP/6-31G**. The pK_a values displayed in this Figure were calculated with a $\Delta G_{solv}(H^+)$ value of –265.74 kcal/mol yielding an RMS deviation of 0.57 pK_a units.

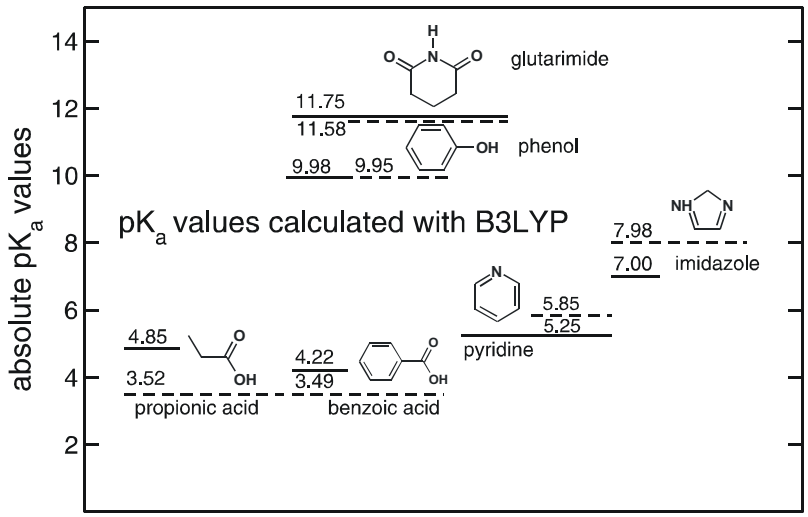

Figure 3.3b. Comparison of experimental (solid line) and calculated (dashed line) pK_a values for six compounds (shown in their neutral state), which represent the six functional groups depicted in Figure 3.1a,b. The computed pK_a values are based on electronic energies E_0 obtained with B3LYP/cc-pVQZ, atomic partial charges from a QC ESP obtained with B3LYP/6-31G** and a $\Delta G_{solv}(H^+)$ value of –265.74 kcal/mol.

Imides, pyridines and imidazoles. The pyridines cover a broad range of more than six pK_a units from 2.84 (3-chloropyridine) to 9.11 (4-amino-pyridine). These large shifts in acidity induced by the different substituents of pyridine are reproduced with high accuracy. The RMS deviation of the six different pyridines is 0.33 (0.57) pK_a units with the largest deviation of 0.50 (0.91) pK_a units for 4-amino-pyridine when estimated with the Becke($^1/_2$)[75] (B3LYP)[76, 77] functional. The raise in acidity induced by chlorine substitution as well as the raise in basicity induced by the amino group (especially in the 4th position) is well reproduced in the computations (see Table 3.1, Figure 3.2a and 3.3a). Inspection of Table 3.2 reveals that B3LYP yields systematically higher PA values than Becke($^1/_2$) for substituted pyridines.

The five substituted imidazoles that were considered in chapter 3.1.1 span a range of five pK_a units. The RMS deviation is 0.56 pK_a units and 0.55 pK_a units using Becke($^1/_2$)[75] and B3LYP[76, 77] functionals, respectively. Independently of the applied DFT functional the largest deviations amounted to nearly 1.00 pK_a units and occurred for imidazole itself. Imidazole has two equivalent protonation sites (Figure 3.1b). To calculate the solvation energies of protonated and deprotonated imidazole I arbitrarily considered one site as titratable and assigned a vdW radius of 1.0 Å to the corresponding proton, while I took the radius 1.2 Å for the other hydrogen. Since I considered only one site titratable, I ignored an entropy contribution of RT ln(2) = 1.02 kcal/mol, which favors the deprotonated state and would shift the pK_a by 0.45 units to more acidic values. This correction reduces the discrepancy between measured and calculated pK_a for imidazole from 0.92 to 0.47 pK_a units but enhances the deviation for the chlorinated imidazole considerably.

3.1.2. Gas phase energetics

The goal of the present study was to establish a protocol that is applicable on a spectrum of chemical compounds with distinct different chemical behaviors. An accurate evaluation of the gas phase is required to ensure that the agreement between computed and measured pK_a values is not the result of an error compensation between gas phase energetics and solvation phase energetics. The directly measurable PA values comprise the enthalpic contribution to ΔG_{gas} (for more information see chapter 2.1.1). Therefore, I calculated PA values on optimized geometries and compared whenever possible to experimental data taken from the NIST webpage (see Table 3.2).[133-138] NIST offers gas phase acidities for 11 of the 13 compounds with a titratable oxygen (carboxylic acids, benzoic acids and phenols),[133, 136-138] which I converted to PA values according to the explanation given in section 2.1.1, while for 9 of the 13 compounds with titratable nitrogen (imides, pyridines and imidazoles) these PA values are directly available.[134, 135] All computed PA values in Table 3.2 and Figure 3.4 and 3.5 were based on DFT using the Becke($^1/_2$)[75] and B3LYP[76, 77] functional.

The agreement of the 21 measured PA values with the corresponding computed PA values is better for QC computations with Becke($^1/_2$) than with B3LYP functional (see Table 3.2). The PA values calculated with Becke($^1/_2$) generally underestimate the experimental PA values. They deviate from measured PA values on the average by –1.88 kcal/mol for the 11 compounds with a titratable oxygen atom and by –0.91 kcal/mol for the 9 compounds with a titratable nitrogen atom. The PA values computed with B3LYP overestimate the 9 measured PA values of compounds with a titratable nitrogen atom on the average by +3.14 kcal/mol, while they scatter around the measured PA values for the 11 compounds with titratable oxygen atom with an RMS deviation of 0.88 kcal/mol. The measured PA values possess an internal uncertainty of about ±2 kcal/mol,[136-138] but depending on the source experimental PA values of substituted pyridines

differ by about 3 kcal/mol (see Table 3.2).[134, 135, 139] Hence, with the exception of the PA values computed with the B3LYP functional for compounds with a titratable nitrogen atom the deviations from the experimental values are well within the error margin of experimental data.

A systematic analysis of computed PA values obtained with different combinations of the DFT functionals (Becke($^1/_2$)[75], B3LYP[76, 77] and BP86[101]) and basis sets (cc-pVQZ, 6-311G++**, cc-pVTZ(-F)++) is provided in Table 3.3 and Figure 3.6. PA values were computed for one member of the six functional groups that were presented in Figure 3.1a,b. Figure 3.6 illustrates that none of the tested combinations of DFT functional and basis sets leads to an agreement between computed and measured PA value for all six compounds. Regarding the three compounds with a titratable oxygen the employed DFT functional (B3LYP, Becke($^1/_2$) and BP86) combined either with the quadruple ζ basis set (cc-pVQZ) or with one of the two triple ζ basis sets (cc-pVTZ(-F)++ or 6-311++G**) yielded PAs that deviate systematically from each other. Figure 3.6 illustrates that B3LYP/cc-pVQZ, BP86/cc-pVQZ and BP86/cc-pVTZ(-F)++ are close to measured PAs of propionic acid, benzoic acid and phenol. Becke($^1/_2$) and B3LYP/cc-pVTZ(-F)++ yielded similar results, which unfortunately underestimated the measured PA values of the three compounds. Differences in the computed PA values due to the employed DFT functional decrease considerably for the depicted imide. Inspection of computed PA values for the two compounds with a titrable nitrogen and a cationic protonated state reveals that Becke($^1/_2$)/cc-pVQZ is in good agreement to measured values.

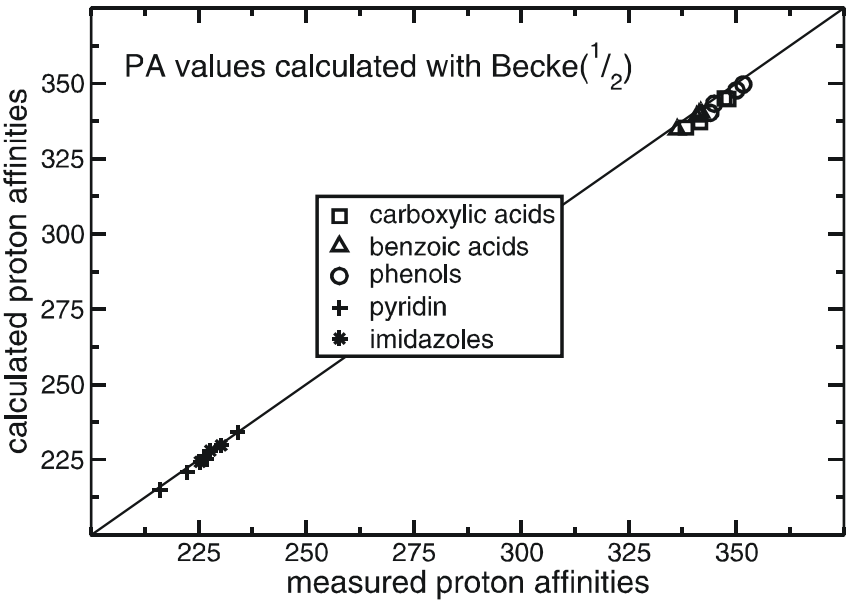

Figure 3.4: Correlation diagram of experimental and calculated PA values for 21 of the 26 compounds listed in Table 3.2. PA values were computed according to eq.2.10 Electronic energies E_0 were obtained with Becke($^1/_2$)/cc-pVQZ. Vibrational energies were calculated the Becke($^1/_2$)/6-31G** level of theory.

Table 3.2. Comparison of calculated PA values based on the QC functionals Becke($^1/_2$) and B3LYP using the cc-pVQZ basis set with experimental data. Computational details are provided in chapter 3.1.2 and 2.7.

substances	formula	Becke($^1/_2$)	B3LYP	measured
carboxylic acids				
propionic acid	C_2H_5-COOH/COO^-	344.84	347.36	348.16[a]
butyric acid	C_3H_7-COOH/COO^-	345.03	347.97	347.26[a]
α-chloropropionic acid	Cl-C_2H_4-COOH/COO^-	337.10	339.71	341.56[a]
β-chloropropionic acid	Cl-C_2H_4-COOH/COO^-	335.31	337.36	338.26[a]
benzoic acids				
benzoic acid	PhCOOH/$PhCOO^-$	338.95	341.81	340.76[b]
p-methylbenzoic acid	4-CH_3-PhCOOH/$PhCOO^-$	340.28	342.36	341.76[b]
m-methylbenzoic acid	3-CH_3-PhCOOH/$PhCOO^-$	339.68	341.71	341.36[b]
p-chlorobenzoic acid	4-Cl-PhCOOH/$PhCOO^-$	334.65	337.69	336.26[b]
phenols				
phenol	PhOH/PhO^-	347.70	350.43	350.06[c]
m-aminophenol	3-NH_2-PhOH/PhO^-	349.66	352.61	351.65[c]
o-aminophenol	2-NH_2-PhOH/PhO^-	348.57	351.11	
m-chlorophenol	3-Cl-PhOH/PhO^-	340.19	342.76	343.96[c]
o-chlorophenol	2-Cl-PhOH/PhO^-	343.24	345.89	344.86[c]
imides				
glutarimide	C_5H_4ONHO/ON^-O	349.48	351.30	
glutaconimide	C_5H_6ONHO/ON^-O	346.81	349.60	
pyridines				
pyridine	$C_5H_5NH^+/C_5H_5N$	220.88	224.78	222.28[d]
2-methylpyridine	2-CH_3-$C_5H_5NH^+/C_5H_5N$	225.21	229.23	226.84[d]
4-methylpyridine	4-CH_3-$C_5H_5NH^+/C_5H_5N$	225.54	229.00	226.39[d]
2-aminopyridine	2-NH_2-$C_5H_5NH^+/C_5H_5N$	226.19	230.01	226.39[d]
4-aminopyridine	4-NH_2-$C_5H_5NH^+/C_5H_5N$	234.20	238.17	234.15[d]
3-chloropyridine	3-Cl-$C_5H_5NH^+/C_5H_5N$	215.12	219.88	215.92[d]
imidazoles				
imidazole	$C_3H_3N_2H_2^+/N_2H$	224.33	227.57	225.33[d]
2-methylimidazole	2-CH_3-$C_3H_3N_2H_2^+/N_2H$	229.75	233.24	230.26[d]
4-methylimidazole	4-CH_3-$C_3H3N_2H_2^+/N_2H$	228.05	231.09	227.73[d]
2-aminoimidazole	2-NH_2.$C_3H3N_2H_2^+/N_2H$	233.04	235.87	
2-chloroimidazole	2-Cl-$C_3H3N_2H_2^+/N_2H$	218.42	222.27	

[a] Reference 136 [b] Reference 137 [c] Reference 138 [d] Reference 135

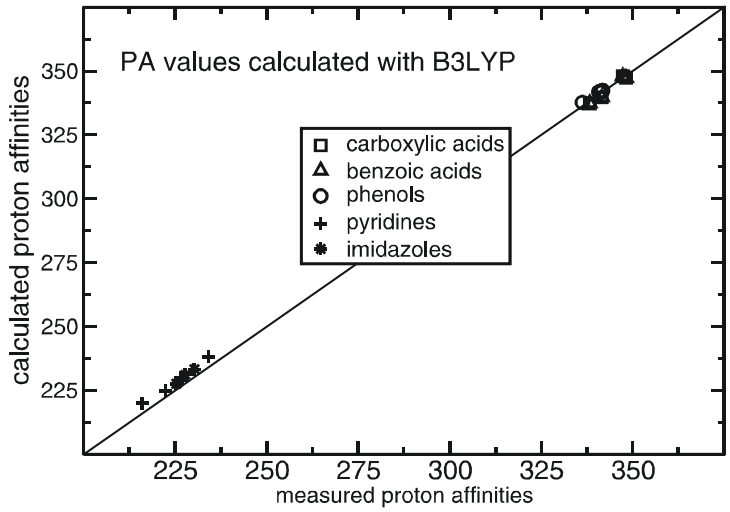

Figure 3.5. Correlation diagram of experimental and calculated PA values for 21 of the 26 compounds listed in Table 3.2. PA values were computed according to eq. 2.10. The computed PA values are based on electronic energies E_0 obtained with B3LYP/cc-pVQZ. Vibrational energies were calculated the Becke($^1/_2$)/6-31G** level of theory.

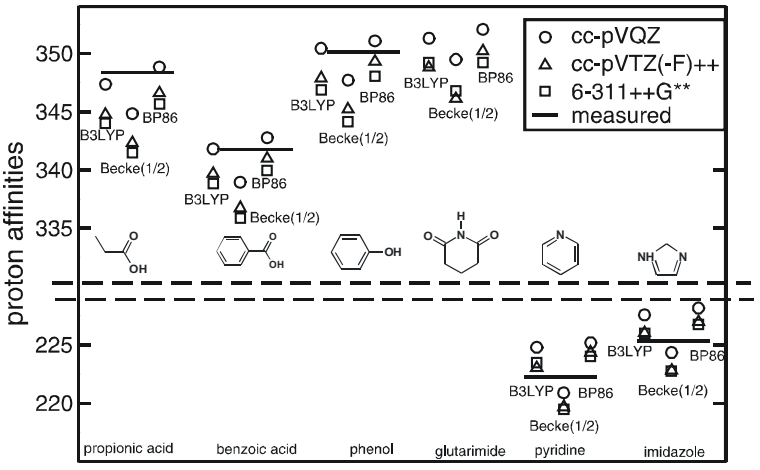

Figure 3.6. Comparison of PA values computed for the six given molecules with the DFT functionals (Becke($^1/_2$),[75] B3LYP[76, 77] and BP86[76, 101]) with experimental data (solid line). For each of the three DFT functionals PA values were calculated using the following basis sets: (cc-pVQZ, cc-pVTZ(-F)++ and the 6-311++G** cc-pVTZ and 6-311++G**. cc-pVQZ, cc-pVTZ(-F)++ are triple basis sets with diffuse and polarization functions, whereas cc-pVQZ is a quadruple basis set that contains only polarization functions. The dashed lines indicate a discontinuity in the scale of PA values between 230 kcal/mol and 330 kcal/mol.

Table 3.3. Comparison of calculated PA values obtained with QC DFT using Becke($^1/_2$),[75] B3LYP[76, 77] and BP86[76, 101] and different basis sets for one member of the functional groups shown in Figure 3.1a,b. A illustration of the results shown here is provided in Figure 3.6.

basis set :		**cc-pvqz**	
QC method:	**Becke$^1/_2$**	**B3LYP**	**BP86**
propionic acid	344.84	347.36	348.85
benzoic acid	338.95	341.81	342.77
phenol	349.66	352.61	351.08
glutarimide	349.48	351.30	352.06
pyridine	220.88	224.78	225.17
imidazole	224.33	227.57	228.15
basis set :		**cc-pvtz(-F)++**	
QC method:	**Becke$^1/_2$**	**B3LYP**	**BP86**
propionic acid	342.35	344.75	346.60
benzoic acid	336.74	339.69	341.00
phenol	345.20	347.89	349.28
glutarimide	346.11	348.82	350.21
pyridine	219.67	223.03	224.34
imidazole	222.81	226.03	226.96
basis set :		**6-311++G****	
QC method:	**Becke$^1/_2$**	**B3LYP**	**BP86**
propionic acid	341.49	344.01	345.68
benzoic acid	335.85	338.84	339.96
phenol	344.16	346.88	348.04
glutarimide	346.78	349.23	350.54
pyridine	219.48	223.48	224.02
imidazole	222.76	225.97	226.77

3.1.3. Estimation of solvation free energies

From solvation energies of a titratable compound I determined the electrostatic free energy contributions only and ignored contributions from van-der-Waals (vdW) interactions and reorganization of the solvent in the presence of a solute molecule, i.e. the hydrophobic effect, which is particularly difficult to evaluate. Unless there are charge specific solvent structures the influence of these interactions cancels in the difference between protonated and deprotonated species. To evaluate the electrostatic energies of solvation I used the Merz–Kollman RESP[69, 70] procedure to fit atomic partial charges from the molecular ESP generated by QC computations on optimized geometries. Table 3.4 lists free electrostatic solvation energies, obtained with the *two-step* procedure based on a QC ESP[109] with Becke($^1/_2$)/6-31G** and B3LYP/6-31G** that was used for the evaluation of pK_a values in chapter 3.1.1. This procedure is explained in chapter 2.7. The solvation energies obtained from that level of theory are compared to results from a QC ESP[109] based on Becke($^1/_2$)/6-31++G** and B3LYP/6-31G++** computations. Hence Table

3.4 documents the influence of diffuse functions on electrostatic solvation free energies. Table 3.4 indicates that the influence of diffuse functions is more pronounced on compounds with a anionic deprotonated state (propionic or benzoic acid) than with a neutral deprotanated state as for instance pyridine or imidazole. For a more detailed analysis on the influence of diffuse functions on computed pK_a values see chapter 3.1.4.

Table 3.4. Solvation free energy differences $\Delta\Delta G_{solv}$, for the 26 titratable compounds employed for pK_a computations and comparison to experimental results. The computed solvation energies are based on atomic partial charges derived from a QC ESP calculated with Becke($^1/_2$)/6-31G** (column 2) and B3LYP/6-31G** (column 4). Column 3 and 4 provides $\Delta\Delta G_{solv}$ values derived from a QC ESP with diffuse functions (6-31++G**) for Becke($^1/_2$) and B3LYP, respectively.

	Becke($^1/_2$)		B3LYP	
substance	6-31G**	6-31++G**	6-31G**	6-31++G**
carboxylic acids				
propionic acid	-69.74	-71.89	-69.08	-71.44
butyric acid	-68.50	-70.79	-67.76	-70.35
2-chloropropionic acid	-63.23	-65.22	-62.54	-64.71
3-chloropropionic acid	-60.93	-63.20	-59.95	-62.66
benzoic acids				
benzoic acid	-64.83	-67.09	-63.56	-66.37
p-methylbenzoic acid	-63.91	-66.82	-63.08	-65.96
m-methylbenzoic acid	-64.43	-66.93	-63.45	-66.12
p-chlorobenzoic acid	-60.72	-62.78	-59.18	-62.11
phenols				
phenol	-64.44	-65.63	-63.40	-65.01
m-aminophenol	-66.12	-67.73	-65.17	-67.00
o-aminophenol	-64.41	-66.04	-63.49	-65.35
m-chlorophenol	-57.29	-58.67	-56.69	-58.28
o-chlorophenol	-61.47	-62.71	-60.53	-62.11
imides				
glutarimide	-63.08	-65.38	-62.05	-64.45
glutaconimide	-63.35	-65.52	-62.20	-64.53
pyridines				
pyridine	-55.95	-55.10	-56.64	-55.54
2-methylpyridine	-51.72	-50.63	-51.97	-51.13
4-methylpyridine	-51.74	-50.68	-52.43	-51.16
2-aminopyridine	-52.01	-51.95	-52.42	-52.22
4-aminopyridine	-48.38	-47.80	-48.93	-48.21
3-chloroyridine	-58.53	-57.49	-58.60	-57.36
imidazoles				
imidazole	-55.99	-55.32	-56.78	-55.90
2-methylimidazole	-50.39	-49.84	-51.38	-50.46
4-methylimidazole	-51.76	-50.96	-52.39	-51.51
2-aminoimidazole	-48.84	-48.01	-49.59	-48.72
2-chloroimidazole	-54.98	-54.57	-55.35	-54.88

3.1.4. Systematic analysis of appropriate conditions of the QC ESP

Computed pK_a values critically depend on electrostatic solvation free energies of the protonated and deprotonated molecules. In the applied approach of the current thesis the atomic partial charges needed to compute solvation energies were derived from the QC ESP[109] in vacuum. Different atomic partial charges were obtained with respect to the applied QC method to estimate the ESP(DFT with B3LYP[76], Becke($^1/_2$)[75, 77] or BP86[76, 101] or Hartree Fock) and the basis set (double ζ, triple ζ, polarisation and diffuse functions). In this section an analysis on different quantum mechanical methods that influence the QC ESP is provided.

The 6-31G** basis set, employed for the QC ESP[109] in the previous chapter with a double set of diffuse functions was augmented to 6-31++G**. The impact due to this basis set modification on pK_a values and electrostatic solvation free energies is provided in the next paragraph for the 26 organic molecules, which were already considered in chapters 3.1.1. In the paragraphs "**Analysis of QC ESP methods on partial atomic charges and solvation energies"** I provide results in terms of partial atomic charges and electrostatic solvation free energies due to modifications in the QC ESP. For one member of each of the six functional groups, which were considered in chapter 3.1.1 I calculated the ESP with the following combinations of QC method and basis sets: HF/6-31G** and HF/6-31++G**; Becke($^1/_2$)/6-31G**, Becke($^1/_2$)/6-31++G**, Becke($^1/_2$)/6-311G** and Becke($^1/_2$)/6-311++G**, B3LYP/6-31G, B3LYP/6-31G**, B3LYP/6-31++G**, B3LYP/6-311G**, B3LYP/6-311++G**.

Computed pK_a values computed with a vacuum ESP using additional diffuse orbitals:

Tables 3.5 lists computed pK_a values for 26 organic compounds, whose electronic energies were obtained either with Becke($^1/_2$)/cc-pVQZ or with B3LYP/cc-pVQZ on optimized geometries. The electrostatic solvation free energies were obtained with atomic partial charges matched with RESP[69, 70] to a QC ESP[109] that was computed either with Becke($^1/_2$)/6-31++G** or with B3LYP/6-31++G**. With an RMS deviation of 0.76 pK_a units and 1.01 pK_a units for Becke($^1/_2$) and B3LYP, respectively, the overall agreement with the measured pK_a values degraded considerably. The reduced overall agreement between computed and measured values is illustrated by the correlation diagrams in Figure 3.7 (Becke($^1/_2$)) and Figure 3.8 (B3LYP).

A comparison on equal footing with the previously presented pK_a values (see chapter 3.1.1) requires the readjustment of $\Delta G_{solv}(H^+)$ so that it accounts for the modified QC ESP.[109] A $\Delta G_{solv}(H^+)$ equal to –260.72 kcal/mol instead of –261.94 kcal/mol minimizes the discrepancy between measured and estimated data if Becke($^1/_2$)/6-31++G** was applied. The value of –264.01kcal/mol instead of –265.74 kcal/mol was calculated, if B3LYP/6-31++G** was used.

Independently of the DFT functional (Becke($^1/_2$)[75] or B3LYP[76, 77]) the pK_a values of carboxylic and benzoic acids are down-shifted using basis sets with diffuse terms, because their $\Delta\Delta G_{solv}$ values increase between 2.0 kcal/mol and 3.0 kcal/mol. This down-shift is only partially compensated using the less negative proton solvation free energy. Inspection of the correlation diagrams (Figure 3.7 and 3.8) reveals that independently of the applied DFT functional, substituted carboxylic and benzoic acids do not meet their corresponding experimental values. Regarding the $\Delta\Delta G_{solv}$ values of substituted phenols the influence of diffuse orbitals is less pronounced. Here, the more negative $\Delta\Delta G_{solv}$ value is almost exactly compensated by the less negative $\Delta G_{solv}(H^+)$ value. The pK_a values of the two imides decrease when diffuse functions were applied to compute the ESP[109] (see Table 3.5). It reveals that switching the basis set from

6-31G** to 6-31++G** yields decreased $\Delta\Delta G_{solv}$ values for pyridines and imidazoles, which would cause decreased pK_a values unless one compensates with a lower $\Delta G_{solv}(H^+)$ value. As the decrement in the solvation energy difference is weaker than the decrement of $\Delta G_{solv}(H^+)$ using diffuse orbitals more basic pyridines and imidazoles were obtained.

Table 3.5. Calculated and measured pK_a values for the 26 considered compounds that were already studied in chapter 3.1.1. Here, computed pK_a values were obtained with partial atomic charges derived from a QC ESP computed with Becke($^1/_2$)/6-31++G** and B3LYP/6-31++G**. Electronic energies and vibrational energies were estimated as in chapter 3.1.1. The pK_a values displayed in this Table were calculated with a $\Delta G_{solv}(H^+)$ value of –260.72 kcal/mol and –265.64 kcal/mol with Becke($^1/_2$) and B3LYP, respectively.

substances	formula	Becke$^1/_2$	B3LYP	measured
carboxylic acids				
propionic acid	C_2H_5-COOH/COO^-	3.50	3.09	4.85[a]
butyric acid	C_3H_7-COOH/COO^-	4.44	4.34	4.85[a]
α-chloropropionic acid	Cl-C_2H_4-COOH/COO^-	2.71	2.41	2.85[a]
β-chloropropionic acid	Cl-C_2H_4-COOH/COO^-	2.88	2.19	4.10[a]
benzoic acids				
benzoic acid	Ph-COOH/$PhCOO^-$	2.70	2.73	4.22[a]
p-methylbenzoic acid	4-CH_3-Ph-COOH/$PhCOO^-$	3.88	3.45	4.37[a]
m-methylbenzoic acid	3-CH_3-Ph-COOH/$PhCOO^-$	3.45	2.85	4.22[a]
p-chlorobenzoic acid	4-Cl-Ph-COOH/$PhCOO^-$	2.71	2.84	3.98[a]
phenols				
phenol	Ph-OH/Ph-O^-	10.21	10.07	9.98[b]
m-aminophenol	3-NH_2-Ph-OH/Ph-O^-	10.10	10.22	9.87[b]
o-aminophenol	2-NH_2-Ph-OH/Ph-O^-	10.55	10.33	9.78[c]
m-chlorophenol	3-Cl-Ph-OH/Ph-O^-	9.81	9.39	9.02[b]
o-chlorophenol	2-Cl-Ph-OH/Ph-O^-	9.08	8.86	8.56[b]
imides				
glutarimide	C_5H_4ONHO/ON^-O	11.71	11.13	11.75[c]
glutaconimide	C_5H_6ONHO/ON^-O	9.63	9.82	9.83[c]
pyridines				
pyridine	$C_5H_5NH^+/C_5H_5N$	5.73	6.32	5.25[d]
2-methylpyridine	2-CH_3-$C_5H_5NH^+/C_5H_5N$	5.63	6.36	5.68[d]
4-methylpyridine	4-CH_3-$C_5H_5NH^+/C_5H_5N$	5.92	6.21	6.02[d]
3-chloropyridine	3-Cl-$C_5H_5NH^+/C_5H_5N$	7.32	7.74	2.84[d]
2-aminopyridine	2-NH_2-$C_5H_5NH^+/C_5H_5N$	10.15	10.78	6.82[d]
4-aminopyridine	4-NH_2-$C_5H_5NH^+/C_5H_5N$	3.26	4.06	9.11[d]
imidazoles				
imidazole	$C_3H_3N_2H_2^+/N_2H$	8.43	8.64	7.00[e]
2-methylimidazole	2-CH_3-$C_3H_3N_2H_2^+/N_2H$	8.39	8.81	7.80[e]
4-methylimidazole	4-CH_3-$C_3H3N_2H_2^+/N_2H$	7.95	8.00	7.45[f]
2-aminoimidazole	2-NH_2-$C_3H3N_2H_2^+/N_2H$	9.47	9.47	8.50[e]
2-chloroimidazole	2-Cl-$C_3H3N_2H_2^+/N_2H$	3.53	3.99	3.55[e]

[a] Reference 3 [b] Reference 40 [c] Calculated using Advanced ChemistryDevelopment (ACD) Software Solaris V4.67 (1994–2003,ACD) [d] Reference 159 [e] Reference 164 [f] Reference 36

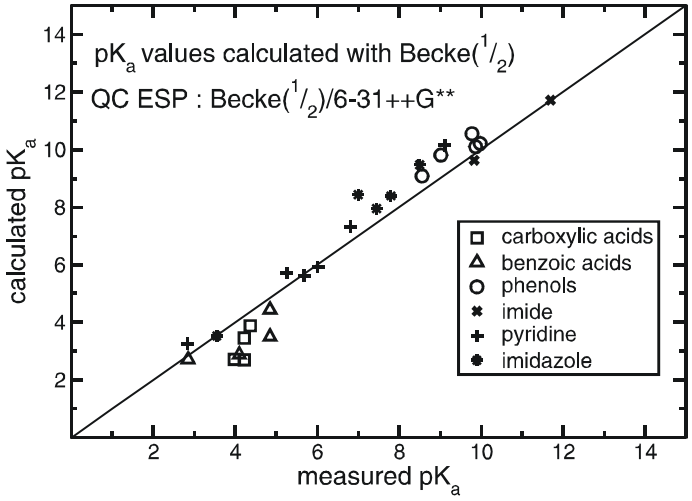

Figure 3.7. Correlation diagram of experimental and calculated pK_a values of the 26 considered compounds listed in Table 3.5. The computed pK_a values are based on electronic energies E_0 obtained with Becke($^1/_2$)/cc-pVQZ. Atomic partial charges used for the computation of solvation energies were calculated on optimized geometries with Becke($^1/_2$)/6-31++G**. The pK_a values displayed in this Figure were calculated with a $\Delta G_{solv}(H^+)$ value of –260.72 kcal/mol yielding an RMS deviation of 0.76 pK_a units.

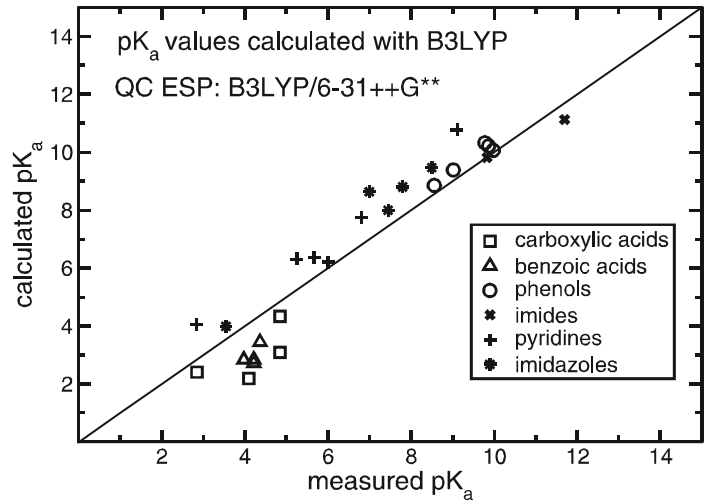

Figure 3.8. Correlation diagram of experimental and calculated PA values of the 26 compounds listed in Table 3.5. The computed pK_a values are based on electronic energies E_0 obtained with B3LYP($^1/_2$)/cc-pVQZ. Atomic partial charges used for computation of solvation energies were calculated on optimized geometries with B3LYP($^1/_2$)/6-31G**. The pK_a values displayed in this Figure were calculated with a $\Delta G_{solv}(H^+)$ value of –264.01 kcal/mol yielding an RMS deviation of 1.03 pK_a units.

Analysis of QC ESP methods on partial atomic charges and solvation energies

Inspection of Table 3.6a-c and Table A.1a-c reveals that enhancement of a basis set as for instance 6-31G** with diffuse functions while conserving the employed QC method yields more polarized charge patterns and more negative electrostatic solvation free energies for the anionic and neutral charged state. This effect is more pronounced for the anionic charge state than for the neutral charge state. Replacement of the DFT functional Becke($^1/_2$)[75] or B3LYP[76, 77] against the Hartree-Fock method while conserving the applied basis set of chapter 3.1.1 (6-31G**) yields similar results (see Table 3.6a-c). Computation of the QC ESP[109] with the Hartree-Fock method and a basis set that includes diffuse functions further amplifies the mentioned effects (see Table 3.6a-c). Partial atomic charges strongly depend on the applied QC method and on polarization and diffuse functions, while the dependence on the number of basis functions in the basis set (double ζ (6-31G) or triple ζ (6-311G)) is small. This holds independently if the DFT functional (Becke($^1/_2$) or B3LYP) or the Hartree-Fock method is applied (see Table 3.6a-c).

3.1.5 Influence of the dielectric constant

Solvation energies and absolute pK_a values presented in chapter 3.1.1, 3.1.3 and 3.1.4 were computed using a solute dielectric constant $\varepsilon = 1$ in the vacuum and in aqueous solution. Computational procedures to determine pK_a shifts and E°_{redox} shifts of titratable or redox-active groups, upon transfer from the solvent phase into the biological environment generally employ an internal dielectric constant of four or higher. I will now inspect the influence of the solute dielectric constant on solvation free energy differences ($\Delta\Delta G_{solv}$) for six organic molecules, which were studied previously (see chapter 3.1.1).

Inspection of Figure 3.9 reveals that upon increasing the solute dielectric constant $\Delta\Delta G_{solv}$ shifts to lower values for compounds with a anionic deprotonated state. The shift is in opposite direction for compounds with a cationic protonated state and a neutral deprotonated state.

Table 3.6a. Electrostatic solvation free energies for the anionic and neutral state and $\Delta\Delta G_{sol}$ values for propionic and benzoic acid derived from a QC ESP with the RESP method. QC ESPs were computed as indicated in column 1.

	propionic acid			**benzoic acid**		
method and basis set	**anion**	**neutral**	**$\Delta\Delta G_{solv}$**	**anion**	**neutral**	**$\Delta\Delta G_{solv}$**
HF/6-31G**	-85.04	-14.02	-71.02	-82.52	-15.44	-67.08
HF/6-31++G**	-87.73	-14.78	-72.95	-84.71	-16.10	-68.61
Becke($^1/_2$)6-31G**	-81.83	-12.09	-69.74	-78.13	-13.30	-64.83
Becke($^1/_2$)6-31++G**	-85.19	-13.26	-71.93	-81.32	-14.23	-67.09
Becke($^1/_2$)6-311G**	-81.73	-12.38	-69.35	-78.71	-13.31	-65.40
Becke($^1/_2$)6-311++G**	-85.10	-13.21	-71.89	-81.52	-14.32	-67.19
B3LYP/6-31G	-82.74	-13.96	-68.78	-78.25	-14.63	-63.62
B3LYP/6-31G**	-80.40	-10.98	-69.42	-75.42	-11.87	-63.55
B3LYP/6-31++G**	-83.73	-12.31	-71.42	-79.25	-12.88	-66.37
B3LYP/6-311G**	-80.06	-11.39	-68.67	-76.31	-12.44	-63.87
B3LYP/6-311++G**	-83.67	-12.28	-71.39	-79.54	-13.01	-66.53

Table 3.6b: Electrostatic solvation free energies for the anionic and neutral state and $\Delta\Delta G_{sol}$ values for glutarimide and phenol derived from a QC ESP with the RESP method. QC ESPs were computed as indicated in column 1.

	phenol			**glutarimide**		
method and basis set	**anion**	**neutral**	**$\Delta\Delta G_{solv}$**	**anion**	**neutral**	**$\Delta\Delta G_{solv}$**
HF/6-31G**	-78.38	-11.64	-66.74	-84.27	-19.51	-64.76
HF/6-31++G**	-80.36	-12.35	-68.01	-88.03	-21.41	-66.62
Becke($^1/_2$)6-31G**	-75.15	-10.71	-64.44	-79.01	-15.93	-63.08
Becke($^1/_2$)6-31++G**	-77.44	-11.81	-65.63	-83.88	-18.51	-65.37
Becke($^1/_2$)6-311G**	-75.91	-10.93	-64.98	-79.23	-16.54	-62.59
Becke($^1/_2$)6-311++G**	-78.02	-11.93	-66.08	-83.49	-18.35	-65.13
B3LYP/6-31G	-75.32	-11.40	-63.92	-80.64	-17.34	-63.30
B3LYP/6-31G**	-73.20	-9.80	-64.40	-76.39	-14.34	-62.05
B3LYP/6-31++G**	-75.54	-10.53	-65.01	-81.68	-17.23	-64.45
B3LYP/6-311G**	-73.95	-9.75	-64.20	-76.75	-15.21	-61.54
B3LYP/6-311++G**	-76.38	-10.23	-66.15	-81.50	-17.32	-64.18

Table 3.6c: Electrostatic solvation free energies for the cationic and neutral state and $\Delta\Delta G_{sol}$ values for pyridine and imidazole derived from a QC ESP with the RESP method. QC ESPs were computed as indicated in column 1.

	pyridine			imidazole		
method and basis set	cation	neutral	$\Delta\Delta G_{solv}$	cation	neutral	$\Delta\Delta G_{solv}$
HF/6-31G**	-64.17	-9.17	-55.00	-70.17	-14.62	-55.50
HF/6-31++G**	-64.19	-9.96	-54.23	-70.15	-15.03	-55.12
Becke($^1/_2$)6-31G**	-63.87	-7.92	-55.95	-69.21	-13.22	-55.99
Becke($^1/_2$)6-31++G**	-63.96	-8.86	-55.09	-69.18	-13.86	-55.32
Becke($^1/_2$)6-311G**	-64.02	-8.23	-55.79	-69.74	-13.35	-56.39
Becke($^1/_2$)6-311++G**	-63.84	-9.00	-54.84	-69.13	-13.73	-55.39
B3LYP/6-31G	-63.70	-8.71	-54.99	-69.27	-13.53	-55.74
B3LYP/6-31G**	-63.56	-6.92	-56.63	-68.66	-11.88	-56.77
B3LYP/6-31++G**	-63.53	-7.99	-55.53	-68.58	-12.68	-55.89
B3LYP/6-311G**	-63.64	-7.44	-56.40	-69.20	-12.21	-56.99
B3LYP/6-311++G**	-63.57	-8.24	-55.33	-69.12	-12.64	-56.48

Table 3.7. The influence of the solute dielectric constant is documented for one member of the six functional groups shown in Figure1a,b.

		$\Delta\Delta G_{solv}$ (kcal/mol)			
compounds	**formula**	**ε =1**	**ε = 2**	**ε= 4**	**ε = 10**
propionic acid	C_2H_5–COOH	-69.74	-68.356	-66.551	-63.961
benzoic acid	Ph–COOH	-64.83	-63.460	-61.542	-58.438
phenol	Ph–OH	-64.44	-63.314	-61.943	-59.935
glutarconimide	$C_5O_2NH_7$	-63.35	-61.199	-59.236	-56.984
pyridine	C_4NH_5	-55.95	-56.664	-57.318	-57.978
imidazole	$C_3N_2H_4$	-55.99	-56.979	-58.763	-60.812

Table 3.8. It is shown here for one member of the six functional groups (shown in Figure1a,b) that the influence of the solute dielectric constant can be partially compensated upon a change of the electrostatic solvation free energies.

$\Delta G_{solv}(H^+)$	**–261.74 kcal/mol**		**–259.50 kcal/mol**	
substances	**ε = 1**	**ε = 4**	**ε = 1**	**ε = 4**
propionic acid	3.98	6.35	5.55	8.14
benzoic acid	3.26	5.68	4.83	7.25
phenol	9.98	11.8	11.55	13.37
glutarconimide	12.29	15.31	13.86	16.88
pyridine	5.26	6.26	6.83	7.83
imidazole	7.88	9.92	9.45	11.49

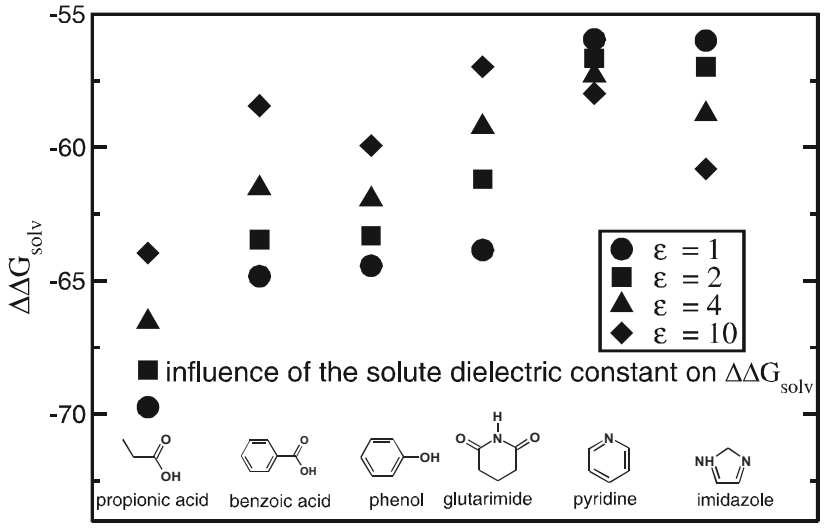

Figure 3.9. Illustration of the influence of the solute dielectric constant on $\Delta\Delta G_{solv}$ for one member of the six functionals groups given in Figure 3.1a,b. An increment of the solute dielectric constant from one to ten yields for the compounds with a deprotonated anionic charge state increased $\Delta\Delta G_{solv}$ values while for compounds with a cationic charge state the effect is vice versa.

3.1.6 Computed pK_a values for methylated phenols

Compute absolute pK_a values for three single methylated phenols diverged stronger from measured values than the compounds, which were considered in chapter 3.1. Table 3.8 reveals that the computed pK_a values for p-methyl, m-methyl and o-methyl phenol of 13.10, 11.06, 11.77 obtained with Becke($^1/_2$) deviate by 2.96, 0.96 and 1.47 pK_a units from measured values, respectively. B3LYP performed slightly better compared to Becke($^1/_2$) regarding the methylated phenols. It yielded pK_a results of 12.10, 10.90 and 11.25 for p-methyl, m-methyl and o-methyl phenol, which implies deviations to measured results of 1.98, 0.82 and 0.95 pK_a units, respectively (see Table 3.8).

The experimental PA values of phenol and o-methyl phenol are nearly identical, whereas the gas phase basicities of m-methyl and p-methyl phenol are increased by 0.72 kcal/mol and 3.30 kcal/mol, respectively. Also PA values diverge the measured pK_a values of the four compounds are virtually identical (see Table 3.8). Hence, $\Delta\Delta G_{solv}$ values of m-methyl and p-methyl phenol must compensate with more negative energies the increased vacuum basicities. Inspection of Table 3.9 reveals that computed PA values based on Becke($^1/_2$) and B3LYP reproduce measured gas phase energetics within the normal error range of the method. Table 3.10 documents that computed $\Delta\Delta G_{solv}$ values for m- and p-methylphenol are not more negative than the $\Delta\Delta G_{solv}$ value of phenol. Consequently estimated free electrostatic solvation energies are the source of error for wrong pK_a values.

The vacuum ESP does not account for the situation in solution:

If we inspect the charge distribution of phenol and compare to the three methylated molecules we notice that the carbon atom, which is bounded covalently to the methyl group, looses between –0.35% and –0.42% of a charge unit in both protonation states, whereas the two neighboring carbon atoms gain negative charge (see Table 8). The CH_3 group itself is slightly negative in the protonated state and significantly negative in the deprotonated state. This charge shift is against the chemical intuition, which states that a methyl group donates a small amount of electrons to its molecular environment. Therefore I assumed that the electronic distribution in vacuum differs from the one in solution and hence the vacuum ESP cannot account for the situation in solution.

To improve the agreement between computed and measured pK_a values regarding methylated phenols I induced the QC ESP of phenol on p-methyl, m-methyl and o-methyl phenol in both protonation states. Hence, I transferred partial atomic charges of phenol and phenoxide to methylated phenols/phenoxides. Atomic partial charges of the methyl group were adopted from the CHARMM22[140] force field. Consequently, the methyl hydrogens assume an atomic partial charge of +0.09. To maintain the total charge of the methylated phenols I added to the methyl carbon charge of –0.27 the atomic charge of the phenol or phenoxide hydrogen, that was replaced by the methyl group (see Table 3.14). With these atomic partial charges I computed the pK_a values depicted in Table 3.12. Table 3.10 reveals that this modification leads to acceptable pK_a values for p-methyl, m-methyl and o-methyl phenol.

Table 3.8. Calculated and measured pK_a values for phenol and p-, m- and o-methylphenol.

substances	formula	Becke($^1/_2$)	B3LYP	measured
phenol	Ph-OH/Ph-O^-	9.98	9.95	9.98[a]
p-methylophenol	4-CH_3-Ph-OH/Ph-O^-	13.10	12.12	10.14[a]
m-methylophenol	3-CH_3-Ph-OH/Ph-O^-	11.06	10.90	10.08[a]
o-methylphenol	2-CH_3-OH/Ph-O^-	11.77	11.25	10.30[a]

[a] Reference 40

Table 3.9. Comparison of measured and calculated PA values for phenol, p-, m- and o-methylphenol.

substances	formula	Becke($^1/_2$)	B3LYP	measured
phenol	Ph-OH/Ph-O^-	347.70	350.43	350.03[a]
p-methylphenol	4-CH_3-Ph-OH/Ph-O^-	349.33	351.24	353.55[a]
m-methylophenol	3-CH_3-Ph-OH/Ph-O^-	348.21	350.78	350.75[a]
o-methylphenol	2-CH_3-OH/Ph-O^-	347.15	349.59	349.95[a]

[a] Reference 138

Table 3.10. Comparison of calculated electrostatic solvation free energies for phenol and p-, m- and o-methylphenol.

		Becke($^1/_2$)	
substances	ΔG_{solv}(neutral)	ΔG_{solv}(anion)	$\Delta\Delta G_{solv}$
phenols			
phenol	-10.94	75.26	-64.32
p-methylphenol	-10.39	-72.42	-62.03
m-methylophenol	-10.40	-73.91	-63.50
o-methylphenol	-9.77	-71.41	-61.64
		B3LYP	
substances	ΔG_{solv}(neutral)	ΔG_{solv}(anion)	$\Delta\Delta G_{solv}$
phenols			
phenol	-9.81	-73.21	-63.40
p-methylphenol	-9.11	-70.41	-61.30
m-methylophenol	-9.10	-71.62	-62.52
o-methylphenol	-8.54	-69.37	-60.83

Table 3.11. Atomic partial charges of phenol and methylated phenol derived from a QC ESP calculated with Becke(1/2)/6-31G** using the RESP method as described in the text (see chapter (2.7).

	charges for the protonated, neutral state				charges for the deprotonated, anionic state			
	phenol	p-methyl	m-methyl	o-methyl	phenol	p-methyl	m-methyl	o-methyl
H1	0.4086	0.4115	0.4122	0.4197				
O1	-0.5717	-0.5709	-0.5704	-0.5587	-0.7458	-0.7407	-0.7469	-0.7086
C1	0.3999	0.3683	0.4259	0.2728	0.5941	0.5636	0.6395	0.4658
C2	-0.3324	-0.2276	-0.3948	0.1341	-0.4062	-0.3795	-0.5737	0.0069
H2	0.1472	0.1685	0.1930		0.0970	0.1045	0.1350	
C2a				-0.3236				-0.2801
H1a1				0.1204				0.0839
H2a2				0.0913				0.0373
C3	-0.0490	-0.2326	0.3051	-0.2217	-0.0531	-0.1985	0.3635	-0.2211
H3	0.1169	0.1512		0.1510	0.0673	0.1014		0.1064
C3a			-0.4295				-0.3741	
H3a1			0.1165				0.0841	
H3a2			0.1258				0.0735	
C4	-0.1869	0.2125	-0.3289	-0.1795	-0.3503	0.0736	-0.4988	-0.3172
H4	0.1211		0.1511	0.1340	0.0924		0.1275	0.0979
C4a		-0.4372				-0.3134		
H4a1		0.1164				0.0651		
H4a2		0.1258				0.0568		
C5	-0.0889	-0.1804	-0.0260	-0.0880	-0.0530	-0.2109	-0.0225	-0.0834
H5	0.1601	0.1456	0.1257	0.1290	0.0673	0.1035	0.0739	0.0762
C6	-0.2479	-0.3381	-0.39299	-0.3263	-0.4067	-0.3879	-0.4649	-0.4148
H6	0.1230	0.1609	0.16128	0.1543	0.0970	0.1057	0.1105	0.1134

Table 3.12. Calculated and measured pK_a values for phenol and p-, m- and o-methylphenol based on the modified procedure to derive atomic partial charges (see chapter 3.1.6).

substances	formula	Becke$^1/_2$	B3LYP	measured
phenol	Ph-OH/Ph-O^-	9.99	9.95	9.98[b]
p-methylophenol	4-CH_3-Ph-OH/Ph-O^-	10.17	10.04	10.14[b]
m-methylophenol	3-CH_3-Ph-OH/Ph-O^-	9.81	9.93	10.08[b]
o-methylphenol	2-CH_3-OH/Ph-O^-	9.73	9.60	10.30[b]

Table 3.13. Solvation free energy differences $\Delta\Delta G_{solv}$, ΔG_{solv}(neutral) ΔG_{solv}(anion) for phenol and p-, m- and o-methylphenol. The computed solvation free energies are based on atomic partial charges obtained with Becke($^1/_2$)/6-31G** and B3LYP/6-31G** and the modified procedure to compute atomic partial charges (see chapter 3.1.6)

	Becke($^1/_2$)		
substances	ΔG_{solv}(neutral)	ΔG_{solv}(anion)	$\Delta\Delta G_{solv}$
phenols			
phenol	-10.71	-75.15	-64.44
p-methylphenol	-11.72	-77.50	-65.78
m-methylophenol	-12.64	-77.85	-65.21
o-methylphenol	-11.81	76.06	-64.25
	B3LYP		
substances	ΔG_{solv}(neutral)	ΔG_{solv}(anion)	$\Delta\Delta G_{solv}$
phenols			
phenol	-9.80	-73.21	-63.40
p-methylphenol	-11.83	-75.72	-63.88
m-methylophenol	-11.81	-75.39	-63.58
o-methylphenol	-11.18	-74.02	-62.84

Table 3.14. Atomic partial charges of phenol and methylated phenol derived from a QC ESP calculated with Becke(1/2)/6-31G** using the modified procedure that is explained in chapter 3.1.6.

	charges for the protonated (neutral state)				charges for the deprotonated (anionic state)			
	phenol	p-methyl	m-methyl	o-methyl	phenol	p-methyl	m-methyl	o-methyl
H1	0.4086	0.4086	0.4086	0.4086				
O1	-0.5717	-0.5717	-0.5717	-0.5717	-0.7458	-0.7458	-0.7458	-0.7458
C1	0.3999	0.3999	0.3999	0.3999	0.5941	0.5941	0.5941	0.5941
C2	-0.3324	-0.3324	-0.3324	-0.3324	-0.4062	-0.4062	-0.4062	-0.4062
H2	0.1472	0.1472	0.1472		0.0970	0.0970	0.0970	0.0970
C2a				-0.1228				
H1a1				0.0900				
H2a2				0.0900				
C3	-0.0490	-0.0490	-0.0490	-0.0490	-0.0531	-0.0531	-0.0531	-0.0531
H3	0.1169	0.1169		0.1169	0.0673	0.0673	0.0673	0.0673
C3a			-0.1531					
H3a1			0.0900					
H3a2			0.0900					
C4	-0.1869	-0.1869	-0.1869	-0.1869	-0.3503	-0.3503	-0.3503	-0.3503
H4	0.1211		0.1211	0.1211	0.0924	0.0924	0.0924	0.0924
C4a		-0.1490						
H4a1		0.0900						
H4a2		0.0900						
C5	-0.0889	-0.0889	-0.0889	-0.0889	-0.0530	-0.0530	-0.0530	-0.0530
H5	0.1601	0.1601	0.1601	0.1601	0.0673	0.0673	0.0673	0.0673
C6	-0.2479	-0.2479	-0.2479	-0.2479	-0.4067	-0.4067	-0.4067	-0.4067
H6	0.1230	0.1230	0.1230	0.1230	0.0970	0.0970	0.0970	0.0970

3.2 Computation of one-electron reduction potentials for oxygen and sulfur centered organic radicals

Computed E^0_{redox} for 21 redox-active organic compounds in water, a protic solvent, as well as acetonitrile (AcN) and N,N-dimethylacetamide (DMAc), which are both aprotic solvents will be presented in the subsequent paragraphs. EA values were evaluated in vacuum by high-level QC methods using G3MP2[78] and DFT with the B3LYP[75, 77] functional. To evaluate one-electron redox potentials, these EA were combined with solvation energies obtained in a two-step computational approach. It will be shown that the DFT functional B3LYP has serious difficulties to account quantitatively for the energetics of electron transfer reactions in the gas phase. Therefore, E^0_{redox} based on the latter method converged less accurately with experimental data. To obtain agreement between measured and calculated one-electron reduction potentials in the considered aprotic solvents the vdW radii of solvation were increased. Electrostatic solvation free energies computed in both dielectric media will be presented in chapter 3.2.3.

3.2.1 E°$_{redox}$ in protic and aprotic solvents

Figure 3.10 depicts eight different redox-active functional groups, which are considered in the present study and are represented by 21 compounds as listed in Table 3.15. For each of the considered 21 organic compounds I computed the one-electron reduction potential, E^0_{redox}, either with G3MP2[78] or with B3LYP[76, 77] in water and AcN/DMAc and compared the values to experimental data if available (see Table 3.15). Redox potentials computed with G3MP2 yielded a RMS deviation of 0.058 V compared to experimental data for the 27 considered organic compounds in water[15, 16, 23-25, 38, 39, 141, 142] and ACN[18, 28, 143] or DMAc.[144] Using the DFT functional B3LYP with the aug-cc-pVTZ basis set involving diffuse functions to all atoms yielded an RMS deviation of 0.131 V when compared to experimental data. Experimental one-electron reduction potentials E^0_{redox} often refer to the normal hydrogen electrode (NHE), whose absolute potential is 4.43 V[5, 55, 90] or to the standard calomel electrode (SCE) where 0.241 V[4, 5] has to be added to obtain NHE values. For B3LYP, a sulfur radius different from the one used with G3MP2 was applied to compensate for systematic errors in EA values (see Table 3.16). The higher discrepancy of computed E^0_{redox} based on B3LYP from measured data compared to one-electron reduction potentials based on G3MP2 is illustrated in the correlation diagram of Figure 3.12 The modified sulfur radius can partially compensate for the errors in the B3LYP energies (see Figure 3.13–3.15). From all redox-active compounds considered here, p-benzoquinone and p-benzodithiyl are the only compounds that have open-shell electronic structures in the anionic charged state. Excluding them from the considered E^0_{redox} values yielded RMS deviations of 0.061V for G3MP2 and 0.113 V for of B3LYP.

Figure 3.10 Redox-active compounds considered in chapter 3.2

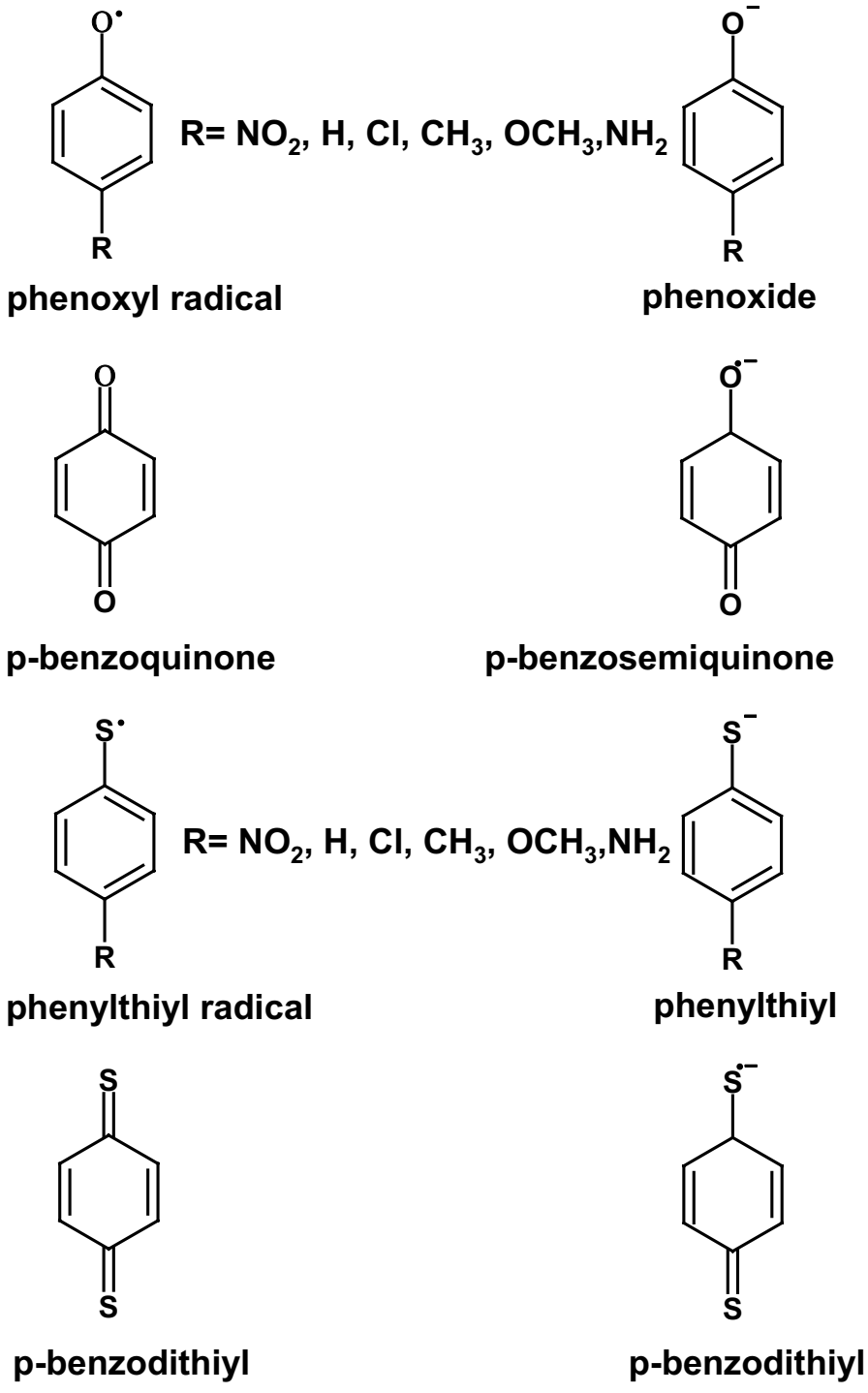

Figure 3.10. (continued):

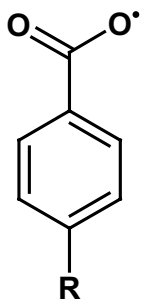

R= H, CH_3

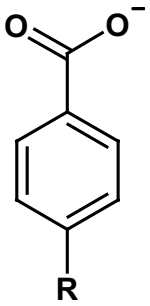

benzoyloxyl radical **benzoic acid anion**

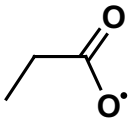

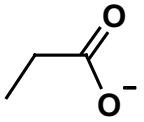

carboxyl radical **carboxyl acid anion**

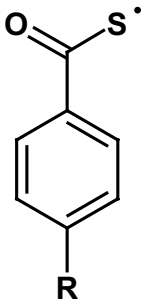

R= H, CH_3,OCH_3

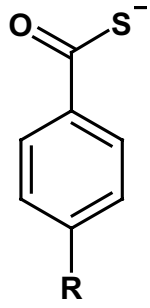

benzoylthiyl radical **benzoylthiyl acid anion**

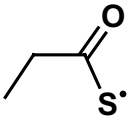

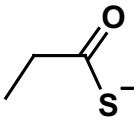

carbthiyl radical **carbthiyl acid anion**

From the 27 experimental E^0_{redox} values, 15 are measured in water[15, 16, 23-25, 38, 39, 141, 142] and 12 in AcN/DMAc.[18, 28, 143] [144] The general agreement between computed and measured redox potentials is documented in the correlation diagram, Figure 3.11. If we do not consider p-amino phenoxyl in AcN the overall RMS deviation for the remaining 26 experimental E^0_{redox} values diminishes from 0.058 V to 0.045 V for the computations with G3MP2.

E°$_{redox}$ in water. The RMS deviation between computed and measured E^0_{redox} values in water considering the 15 measured[15, 16, 23-25, 38, 39, 141, 142] compounds is 0.053 V for computations with G3MP2 (Table 3.15). Using B3LYP instead of G3MP2 the corresponding RMS deviation is 0.145 V (see Table 3.15) Computed RMS deviations are based on averaged experimental data when available as it is for instance for p-substituted phenoxyl radicals. Inspection of Table 3.15 and Figure 3.11 reveals that computed E°$_{redox}$ values scatter evenly around the corresponding measured values, without systematic deviations. Since discrepancies between 30 mV and 70 mV in measured E°$_{redox}$ values determined in different labs are considered as a good agreement,[16, 38] one can be faithful that the computed one-electron reduction potentials based on G3MP2 in water displayed in Table 3.15 generally agree with experimental data (see Table 3.15).

Due to a lack of direct experimental data, Zhao et al.[23] estimated the E^0_{redox} of the benzoyloxyl, carboxyl and carbthiyl radicals from measured oxygen-hydrogen and sulfur-hydrogen bond dissociation energies to be 2.0 V, 1.9 V and 1.1 V, respectively. Subsequently, they measured E^0_{redox} for the carbthiyl radical directly yielding a considerably higher value of 1.21 V.[24, 25] The computed E^0_{redox} for the carbthiyl radical matches with the latter experimental value within 10 mV. Table 3.15 also reveals that the computed E^0_{redox} of the substituted benzoylthiyls,[23-25] which are the sulfur analogs of benzoyloxyl radicals, are in a good agreement with experimental data. Hence, I am confident that the computed E^0_{redox} values of 2.27 V and 2.32 V for the benzoyloxyl and carboxyl radical, respectively, are trustworthy. Considering EA values will further support the reliability of the computed one-electron reduction potentials.

Table 3.15. Comparison of directly measured and calculated redox potentials E^0_{redox} for the functional groups depicted in Figure 3.10 using the QC method G3MP2 and B3LYP as explained in text. E^0_{redox} values were computed for the protic solvent water and the aprotic solvents acetonitrile (AcN) and N,N-dimethylacetamide (DMAc). The latter solvent was employed for the $E°_{redox}$ measurements of the benzoylthiyl and carbthiyl radicals. I do not discriminate between the two aprotic solvents in the computations, since they have virtually the same dielectric constant of ε = 37.5. However, I use solute vdW radii as discussed in the method section that differ for the protic (water) and the aprotic (AcN/DMAc) solvents. Within each group of compounds the entries are ordered from top to bottom with descending computed E^0_{redox} value. Experimental E^0_{redox} values are listed if available. E^0_{redox} values estimated from bond dissociation energies are listed in the footnote.

		$E°_{redox}$ [V] in water		
substances	**formula**	**measured**	**G3MP2**	**B3LYP**
phenoxyl radical				
p-nitro-phenoxyl-radical	4-NO_2-Ph-$O^{\bullet}/O^-$	1.28[a]/1.23[b]	1.330	1.330
phenoxyl-radical	4-H-Ph-$O^{\bullet}/O^-$	0.86[a]/0.79[b]	0.906	0.758
p-chloro-phenoxyl-radical	4-Cl-Ph-$O^{\bullet}/O^-$	0.85[a]/0.80[b]	0.885	0.687
p-methyl-phenoxyl-radical	4-CH_3-Ph-$O^{\bullet}/O^-$	0.71[a]/0.68[b]	0.683	0.480
p-methoxy-phenoxyl-radical	4-CHO_3-Ph-$O^{\bullet}/O^-$	0.58[a]/0.54[b]/0.44[c]	0.460	0.305
p-amino-phenoxyl-radical	4-NH_2-Ph-$O^{\bullet}/O^-$	0.24[d]/0.217[e]	0.225	-0.059
p-benzoquinone				
p-benzoquinone	O=Ph=O/O=Ph-$O^{\bullet-}$	0.10[f]/0.11[g]	0.110	0.372
phenylthiyl radical				
p-nitro-phenylthiyl-radical	4-NO_2-Ph-$S^{\bullet}/S^-$		0.970	1.028
phenylthiyl-radical	4-H-Ph-$S^{\bullet}/S^-$	0.69[e]	0.746	0.693
p-chloro-phenylthiyl-radical	4-Cl-Ph-$S^{\bullet}/S^-$		0.727	0.689
p-methyl-phenylthiyl-radical	4-CH_3-Ph-$S^{\bullet}/S^-$	0.64[e]	0.582	0.587
p-methoxy-phenylthiyl-radical	4-CHO_3-Ph-$S^{\bullet}/S^-$	0.57[e]	0.472	0.419
p-amino-phenoxyl-radical	4-NH_2-Ph-$S^{\bullet}/S^-$	0.36[e]	0.450	0.300
p-benzodithiyl				
p-benzodithiyl	S=Ph=S/-$S^{\bullet-}$		0.454	0.862
benzoyloxyl radical				
benzoyloxyl radical*[1]	Ph-$COO^{\bullet}/O^-$		2.326	1.915
p-methyl-benzoyloxyl-radical	CH_3-Ph-$COO^{\bullet}/O^-$		2.240	1.819
carboxyl radical				
propionic acid radical*[1]	C_2H_5-$COO^{\bullet}/O^-$		2.273	1.905
benzoylthiyl radical				
benzoylthiyl radical	Ph-$COS^{\bullet}/S^-$	1.21[h]	1.220	1.196
p-methyl-benzoylthiyl-radical	CH_3-Ph-$COS^{\bullet}/S^-$	1.19[i]	1.210	1.120
p-methoxy-benzoylthiyl-radical	CH_3O-Ph-$COS^{\bullet}/S^-$	1.17[i]	1.110	1.092
carbthiyl radical				
thiopropanoic acid radical*[1]	C_2H_5-$COS^{\bullet}/S^-$	1.22[j]	1.207	1.254

Table 3.15 (continued)

substances	formula	$E°_{redox}$ [V] in ACN/DMAc measured	G3MP2	B3LYP
phenoxyl radical				
p-nitro-phenoxyl-radical	4-NO_2-Ph-$O^{\bullet}/O^-$	0.981[k]	1.018	1.000
phenoxyl-radical	4-H-Ph-$O^{\bullet}/O^-$	0.461[k]	0.503	0.334
p-chloro-phenoxyl-radical	4-Cl-Ph-$O^{\bullet}/O^-$		0.522	0.327
p-methyl-phenoxyl-radical	4-CH_3-Ph-$O^{\bullet}/O^-$	0.279[k]	0.305	0.105
p-methoxy-phenoxyl-radical	4-CHO_3-Ph-$O^{\bullet}/O^-$		0.060	-0.089
p-amino-phenoxyl-radical	4-NH_2-Ph-$O^{\bullet}/O^-$		–0.180	-0.454
p-benzoquinone				
p-benzoquinone	O=Ph=O/O=Ph-$O^{\bullet-}$	–0.270[l]	–0.260	-0.001
phenylthiyl radical				
p-nitro-phenylthiyl-radical	4-NO_2-Ph-$S^{\bullet}/S^-$	0.701[m]	0.735	0.792
phenylthiyl-radical	4-H-Ph-$S^{\bullet}/S^-$	0.401[m]	0.444	0.398
p-chloro-phenylthiyl-radical	4-Cl-Ph-$S^{\bullet}/S^-$	0.471[m]	0.460	0.415
p-methyl-phenylthiyl-radical	4-CH_3-Ph-$S^{\bullet}/S^-$	0.311[m]	0.298	0.283
p-methoxy-phenylthiyl-radical	4-CHO_3-Ph-$S^{\bullet}/S^-$	0.181[m]	0.202	0.102
p-amino-phenoxyl-radical	4-NH_2-Ph-$S^{\bullet}/S^-$	–0.099[m]	0.094	-0.054
p-benzodithiyl				
p-benzodithiyl	S=Ph=S/-$S^{\bullet-}$		0.201	0.648
benzoyloxyl radical				
benzoyloxyl radical*[1]	Ph-$COO^{\bullet}/O^-$		1.880	1.480
p-methyl-benzoyloxyl-radical	CH_3-Ph-$COO^{\bullet}/O^-$		1.795	1.411
carboxyl radical				
propionic acid radical*[1]	C_2H_5-$COO^{\bullet}/O^-$		1.761	1.175
benzoylthiyl radical				
benzoylthiyl radical	Ph-$COS^{\bullet}/S^-$	0.940[n] *2	0.910	0.875
p-methyl-benzoylthiyl-radical	CH_3-Ph-$COS^{\bullet}/S^-$		0.842	0.767
p-methoxy-benzoylthiyl-radical	CH_3O-Ph-$COS^{\bullet}/S^-$		0.775	0.774
carbthiyl radical				
thiopropanoic acid radical*[1]	C_2H_5-$COS^{\bullet}/S^-$	0.820[n] *2	0.860	0.920

[a] Reference 16 [b] Reference 38 [c] Reference 15 [d] Reference 141 [e] Reference 142 [f] Reference 27 [g] Reference 39 [h] Reference 23 [i] Reference 24 [j] Reference 25 [k] Reference 18 [l] Reference 28 [m] Reference 143 [n] Reference 144

*[1] Estimation of bond dissociation energies (indirect measurement as discussed in text) yield E^0_{redox} values in water of 2.0 and 1.9 and 1.1 V for the radicals benzoyloxyl, carboxyl, and carbthiyl, respectively.

*[2] E^0_{redox} in DMAc. E^0_{redox} values were computed for the protic solvent water and the aprotic solvents AcN and DMAc. The latter solvent was employed for the E^0_{redox} measurements of the benzoylthiyl and carbthiyl radicals. We do not discriminate between the two aprotic solvents in the computations, since they have virtually the same dielectric constant of ε = 37.5.

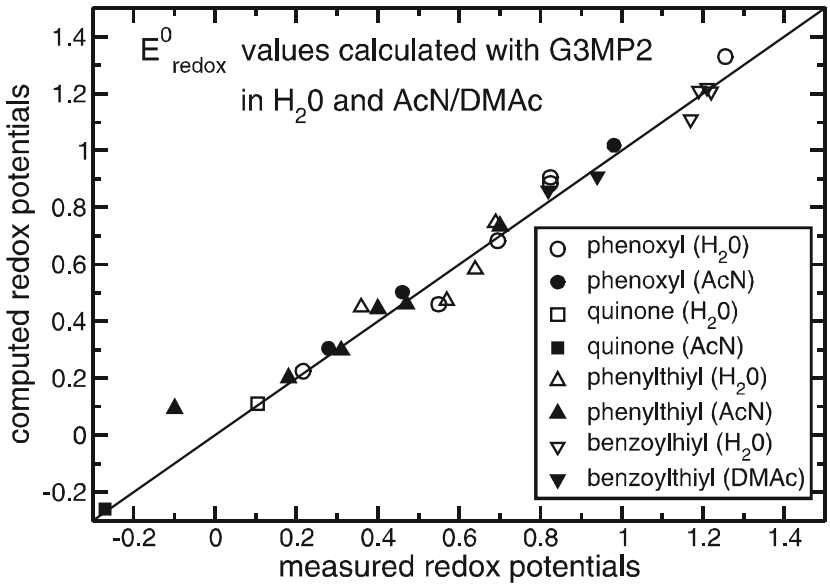

Figure 3.11: Correlation diagram of experimental and calculated redox potentials of the redox-active groups considered in the present work. Optimized geometries, electronic and vibrational energies in the gas phase were computed with G3MP2 implemented in GAUSSIAN03.[131] Solvation energies were calculated using atomic partial charges obtained with B3LYP/6-31G**. As stated in the text (see also chapter 2.7) I computed solvation free energies with a different set of vdW radii for each solvent type (H_2O and AcN/DMAc). For p-substituted phenoxyl radicals and p-benzoquinone I used the average value of independent measurements (see Table 3.15). The RMS deviation for 27 out of 42 calculated E^0_{redox} values equals 0.058 V.

E°$_{redox}$ in acetonitrile and N,N-dimethylacetamide. The E^0_{redox} of twelve of the 21 considered redox-active compounds were measured in the aprotic solvents AcN or DMAc. The latter solvent was used to measure E^0_{redox} for benzoylthiyl and carbthiyl. Comparison of experimental with computed E^0_{redox} values based on G3MP2[78] yields an RMS deviation of 0.063 V. Similar as in the case of water the computed redox potentials scatter evenly around the measured values and exhibit no systematic deviation (Figure 3.11 and Table 3.15). Computed E^0_{redox} values based on B3LYP/aug-cc-pVTZ yielded an RMS deviation of 0.111 V (see Figure 3.13 and 3.15 and Table 3.15) are less successful.

The computed E°$_{redox}$ of p-amino phenylthiyl exceeds the measured value by 193 mV. Table 3.15 reveals that the E^0_{redox} values of phenylthiyl, p-methyl-, p-methoxy- and p-amino phenylthiyl are down-shifted changing the solvent from water to AcN by 0.29 V, 0.33, 0.39 V and 0.56 V, respectively. Interestingly, the solvent down-shift of E^0_{redox} for p-amino phenylthiyl in AcN is much larger than for the other three phenylthiyl radicals. On the other hand, the computed solvent down-shift of E^0_{redox} for p-amino phenylthiyl changing from water to AcN is only 0.356 V and

thus consistent with the other three measured solvent downshifts. If I do not consider p-amino phenylthiyl in the evaluation of RMS deviation its value would be reduced from 0.06 to 0.03 V.

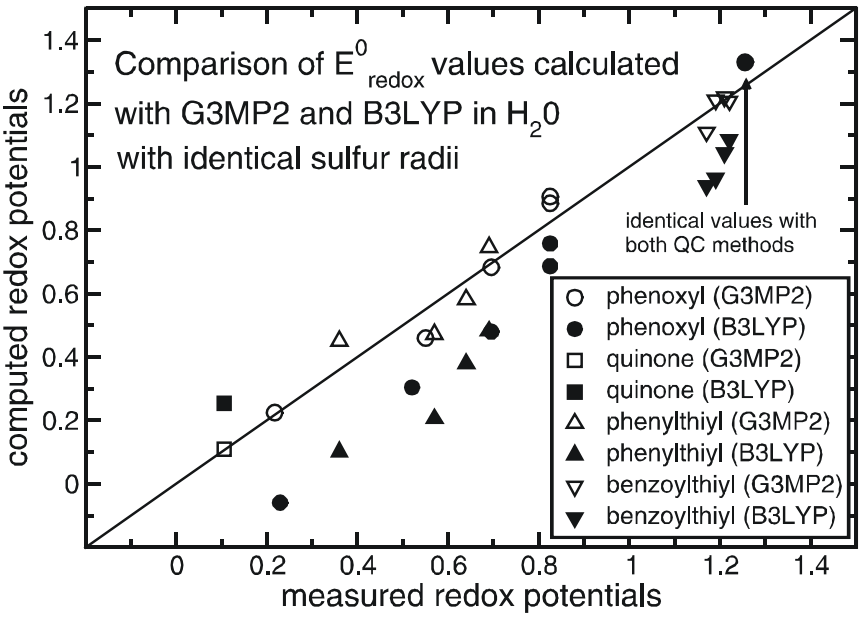

Figure 3.12. Correlation diagram of experimental and computed (G3MP2 and B3LYP) E^0_{redox} in water of the redox-active compounds considered in chapter 3.2. Electronic energies with B3LYP employed the aug-cc-pVTZ basis set. Independent of the applied QC method for electronic energies solvation free energies were calculated with atomic partial charges obtained with B3LYP/6-31G**. Solvation energies using B3LYP geometries were computed with identical vdW radii used for G3MP2 geometries in the protic solvent (H_2O) and aprotic solvents acetonitrile (AcN) and N,N-dimethylacetamide (DMAc).

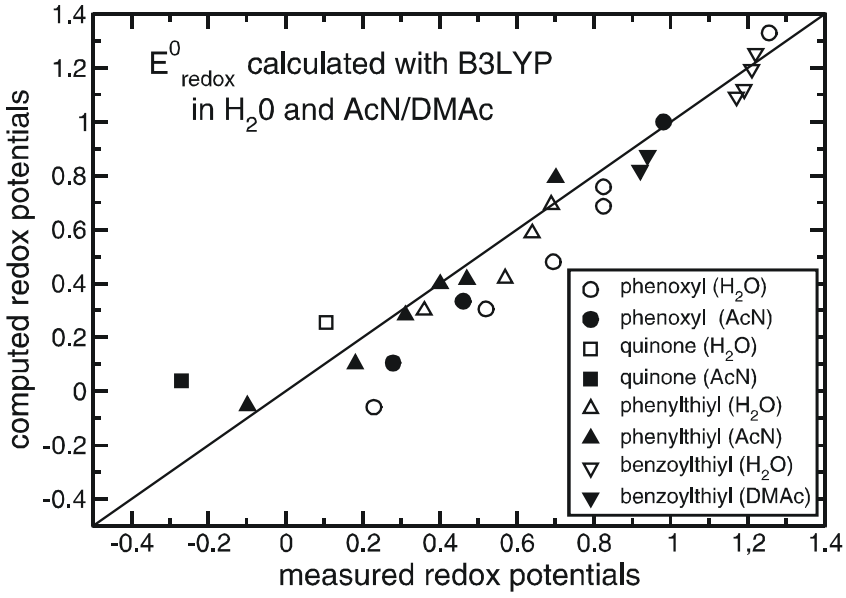

Figure 3.13. Correlation diagram of experimental and calculated redox potentials of the redox-active groups considered in chapter 3.2. Vacuum electron affinities were estimated using B3LYP/aug-cc-pVTZ. Solvation energies were calculated with atomic partial charges obtained with B3LYP/6-31G**. Solvation energies were computed with a sulfur vdW radius of 1.80 Å in the protic solvent water and 2.00 Å in the aprotic solvents acetonitrile (AcN) and N,N-dimethylacetamide (DMAc) and otherwise identical vdW radii used with G3MP2 (see chapter 2.7). All single point computations employed B3LYP/6-31G** geometries. For p-substituted phenoxyl radicals and p-benzoquinone I used the average value of independent measurements (see Table 3.15). The overall RMS deviation for the 27 out of 42 considered E^0_{redox} equals 0.131 V.

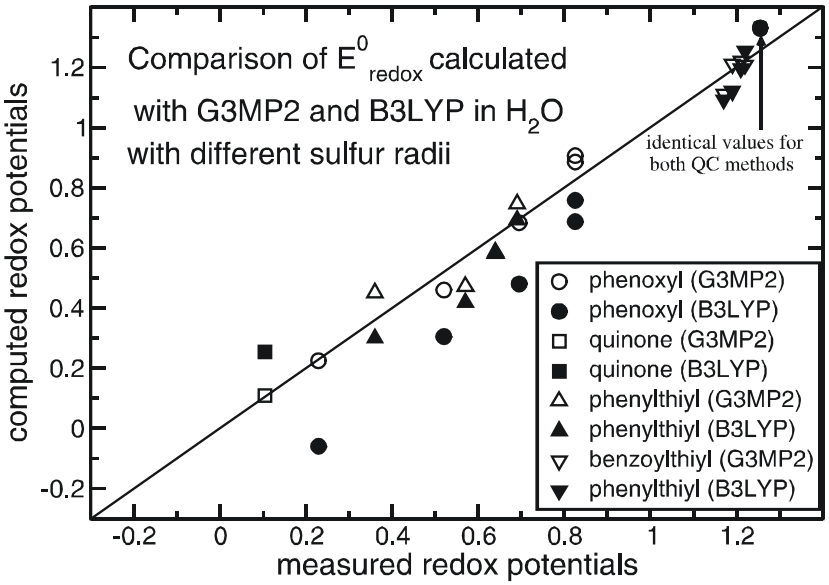

Figure 3.14: Correlation diagram of experimental and calculated redox potentials in water of the redox-active compounds considered in this work. Figure 3.14 correlates computed redox potentials based on G3MP2 electron affinities and computed redox potentials based on DFT B3LYP using the aug-cc-pVTZ basis set with experimental results. Solvation energies for B3LYP geometries were computed with a sulfur vdW radius of 1.80 Å in the protic solvent water and otherwise identical vdW radii used with G3MP2 (see chapter 2.7).

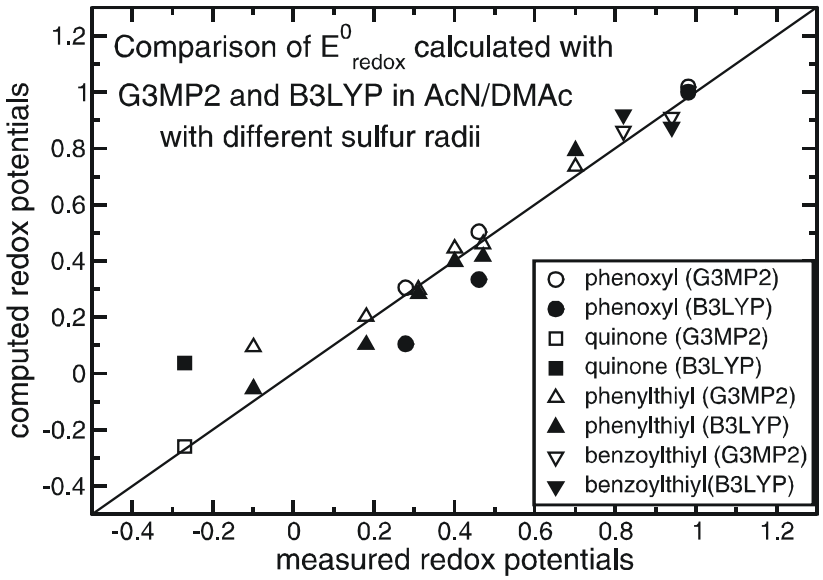

Figure 3.15: Correlation diagram of experimental and calculated redox potentials in acetonitrile (AcN) and N,N-dimethylacetamide (DMAc) of the redox-active compounds. Figure 3.15 correlates computed redox potentials based on G3MP2 electron affinities and computed redox potentials based on DFT B3LYP (using the aug-cc-pvTZ basis set) with experimental results. Solvation energies based on B3LYP geometries were computed with a sulfur radius of 2.00 Å. and otherwise identical vdW radii used with G3MP2 (see chapter 2.7).

3.2.2 Estimation of EA values

EA values were computed for the 21 organic compounds according to the definition given in chapter 2.1.2. I computed EA values using the QC method G3MP2[78] and compared with experimental data. I also computed adiabatic EA values for the same set of compounds using the B3LYP functional (see Table 3.16). These computations were based on molecular geometries optimized with B3LYP/6-31G** using GAUSSIAN03.[131] Experimental EA values are available on the NIST webpage[133] for seven redox-active compounds, namely, phenoxyl,[138, 145, 146] p-chlorophenoxyl,[138] p-methylphenoxyl,[138] p-benzoquinone,[147-149] phenylthiyl,[146, 150] benzoyloxy[138] and carbthiyl (see Table 3.16).[136, 151] These EA values match with the corresponding computed G3MP2 values yielding an RMS deviation of 54 meV. The RMS deviation between measured and computed EA values based on B3LYP is 210 meV. If I neglect p-benzoquinone the EA values computed with G3MP2 and B3LYP match the measured values with RMS deviations of 58 meV and 200 meV, respectively.

All considered redox active compounds are radicals in the uncharged state, except for p-benzoquinone and p-benzodithiyl, which are radicals in the anionic state. Interestingly, B3LYP overestimates the EA values of p-benzoquinone considerably, whereas G3MP2 yields also in this case good agreement with the measured value.[147-149] Hence, I conclude that the EA value of benzodithiyl obtained with G3MP2 is reliable but not the EA value provided by B3LYP.

The orientation of the NH_2 group of p-amino phenoxyl varies with the redox state in gas phase computations performed with G3MP2. In the oxidized radical state, the amino group hydrogen atoms are in the aromatic ring plane, while in the negative none-radical state they are rotated by 90° in the out-of-plane conformation. Interestingly, computations with B3LYP favor the in plane conformation of the amino group hydrogen atoms in both redox states. Regarding the orientation of the NH_2 group of p-amino phenylthiyl both QC methods favor the in plane conformation independently of the considered redox state.

For some open-shell molecular species geometry optimization may lead to different electronic states and as a consequence to slightly different geometries depending on the applied QC method. To these molecular compounds belong the charge neutral radicals of carbonic acids, which can adopt the electronic state $^2A_1$ with a symmetric pair of C–O bonds or the $^2A'$ state with unequal C–O bond lengths (broken symmetry).[152, 153] For the carbonic acids benzoyloxyl and propanoyloxyl radical (Fig. 3.10) considered in the present study, both applied QC methods (G3MP2[78] and B3LYP[76, 77]) yielded with geometry optimization broken symmetry, which means that the unpaired electron is distributed unevenly between the two oxygen atoms of the COO group. In the computation of vibrational states no imaginary frequencies were observed, which means that the true energy minima were found.

Table 3.16. Comparison of directly measured and calculated EA values. EA values were computed with G3MP2 and B3LYP/aug-cc-pVTZ. For B3LYP single point calculations I used coordinates obtained at the B3LYP/6-31G** level of theory.

		EA [eV]	
substances	**measured**	**G3MP2**	**B3LYP**
phenoxyl radical			
4-NO2-Ph-O$^{\bullet}$/O^{-}		3.453	3.425
4-H-Ph-O$^{\bullet}$/O^{-}*	2.25[a], 2.30[b], ≤ 2.36[c]	2.379	2.210
4-Cl-Ph-O$^{\bullet}$/O^{-}*	2.58[b]	2.626	2.446
4-CH_3-Ph-O$^{\bullet}$/O^{-}*	2.17[b]	2.251	2.060
4-CHO_3-Ph-O$^{\bullet}$/O^{-}		2.084	1.863
4-NH_2-Ph-O$^{\bullet}$/O^{-}		1.923	1.643
p-benzoquinone			
O=Ph=O/O=Ph-O$^{\bullet-}$	1.86[d], 1.91[e], 1.99[f]	1.917	2.178
phenylthiyl radical			
4-NO2-Ph-S$^{\bullet}$/S^{-}		3.339	3.256
4-H-Ph-S$^{\bullet}$/S^{-}*	2.46[g], ≤ 2.47[c]	2.515	2.287
4-Cl-Ph-S$^{\bullet}$/S^{-}		2.754	2.502
4-CH_3-Ph-S$^{\bullet}$/S^{-}		2.434	2.180
4-CHO_3-Ph-S$^{\bullet}$/S^{-}		2.326	2.050
4-NH_2-Ph-S$^{\bullet}$/S^{-}		2.241	1.870
p-benzodithiyl			
S=Ph=S/S=Ph-S$^{\bullet-}$		2.656	2.964
benzoyloxyl radical:			
Ph-COO$^{\bullet}$/O^{-}*	3.75[b]	3.813	3.427
CH3-Ph-COO$^{\bullet}$/O^{-}		3.76	3.358
carboxyl radical			
C2H5-COO$^{\bullet}$/O^{-}*	3.43[h], 3.40[i]	3.468	3.157
benzoylthiyl radical:			
Ph-COS$^{\bullet}$/S^{-}		3.08	2.904
CH3-Ph-COS$^{\bullet}$/S^{-}		3.033	2.847
CH3O-Ph-COS$^{\bullet}$/S^{-}		3.008	2.799
carbthiyl radical			
C2H5-COS$^{\bullet}$/S^{-}		2.868	2.750

[a] Reference 145 [b] Reference 138 [c] Reference 146 [d] Reference 147 [e] Reference 148 [f] Reference 149 [g] Reference 150 [h] Reference 136 [i] Reference 151

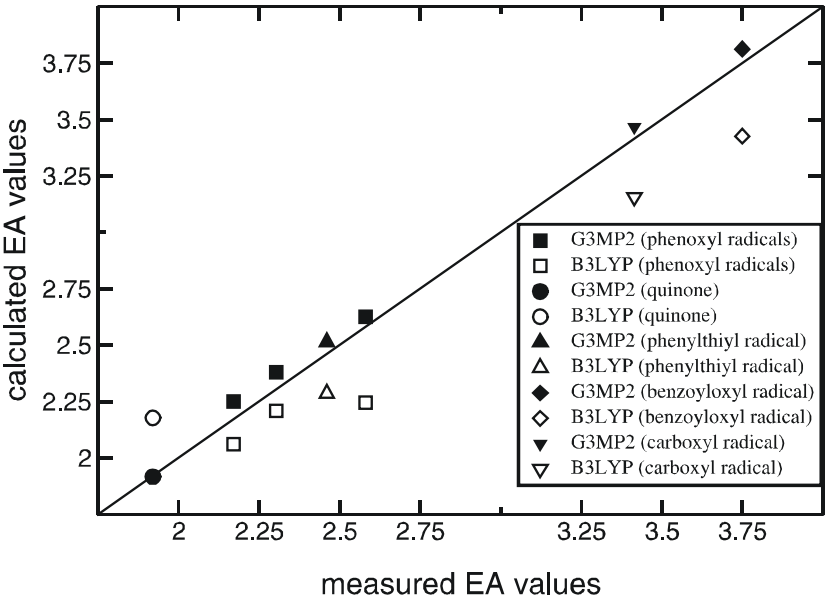

Figure 3.16. Correlation of measured and calculated EA values for seven of the 21 compounds listed in Table 3.16. For the phenoxyl radical, benzoquinone and the phenylthiyl radical I used the average of the experimental data (see Table 3.16). EA values were computed as described in the text (see also sections 2.1.2 and 2.7). The RMS deviations between computed and experimental data amount to 54 meV for G3MP2 and 210 meV for B3LYP.

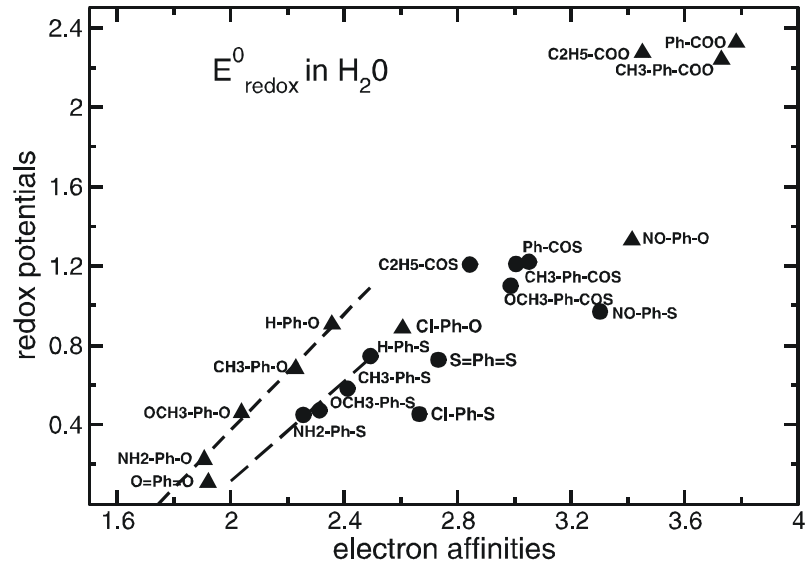

Figure 3.17: Calculated EA values and computed redox potentials of 21 redox-active compounds in water are plotted Triangles represent redox-active compounds with an oxygen centered radical and circles redox-active compounds with an sulfur centered radical. Figure 3.17 illustrates the redox potentials shift induced by the aqueous solution.

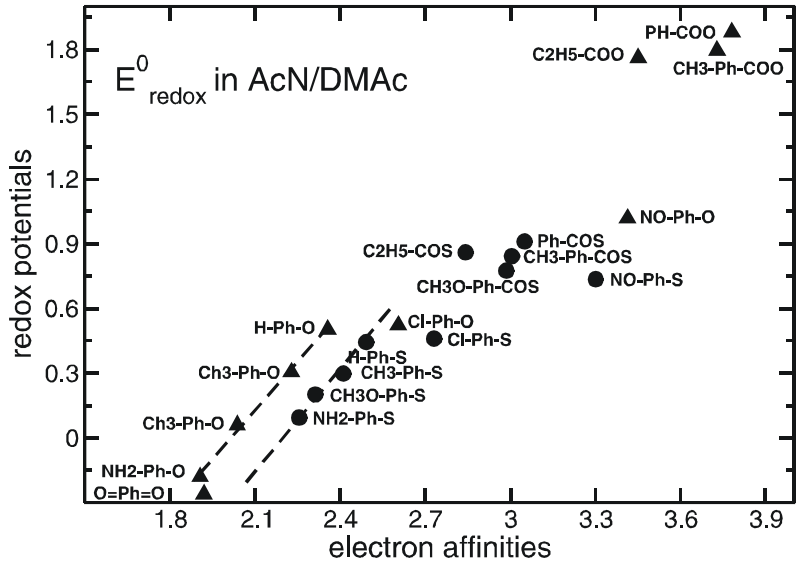

Figure 3.18: Calculated EA values and computed redox potentials of 21 redox-active compounds in AcN/DMAc are plotted. Triangles represent redox-active compounds with an oxygen centered radical and circles redox-active compounds with a sulfur centered radical. Figure 3.18 illustrates the redox potential shift induced by the considered aprotic solvents.

3.2.3 Solvation free energies

To evaluate the contribution of solvation to the redox potential of a redox-active compound, I computed the electrostatic energy difference between gas phase and solution phase for both redox states by solving the Poisson equation for a continuum dielectric medium with $\varepsilon = 1$ in the solute volume and $\varepsilon_{solv} > 1$ and vanishing ionic strength in the solvent. In combination with the G3MP2 QC method a single set of vdW radii for solute atoms was sufficient to estimate the electrostatic solvation free energies in water for all considered redox-active compounds. These are the same vdW radii used for pK_a computations (see chapter 3.1 and 2.7),[41] with the exception that the somehow artificial discrimination between aliphatic and none-aliphatic carbons is dropped in this chapter. The adiabatic EA values computed with B3LYP for sulfur-centered radicals were by more than 200 meV lower than the corresponding experimental values (see Table 3.16). To regain agreement between measured and B3LYP computed E^0_{redox} values of sulfur-centered radicals in water the deviations in EA can be partially compensated by using a smaller sulfur radius of 1.80 Å for the evaluation of the solvation energies. In AcN and DMAc redox-active compounds with G3MP2 geometries were solvated with an enhanced set of vdW radii of solvation. This enhancement was about 15% for all atoms but the hydrogen atoms, where the vdW radius applied in water was used. Again, to obtain agreement between computed and measured E^0_{redox} values for sulfur-centered radicals in AcN/DMAc I decreased the sulfur vdW radius from 2.3 Å used for G3MP2[78] to 2.0 Å for B3LYP[75, 77] geometries (see Figure 3.13 and 3.15).

Solvation energies in different solvents.

Computations with solute atom vdW radii as used for water, yielded E^0_{redox} values for AcN/DMAc, which are on the average only between 60 to 100 mV below the corresponding $E°_{redox}$ values for water, while the dependence of $\Delta\Delta G_{solv}$ values on the solvent probe radius is indeed negligible (see Table 3.18), while in AcN/DMAc the experimental E^0_{redox} values are about 300 mV to 400 mV below the corresponding values for water (Table 3.15). Hence, the large decrease in the dielectric constant from $\varepsilon_{H2O} = 80$ to $\varepsilon_{AcN} = 37.5$, which diminishes in particular the stabilization of the anionic solute redox state, can account only for a fraction of the observed decrease in the experimental E^0_{redox} values. Thus, based on the rational given above, we increased the vdW radii of the non-hydrogen solute atoms for the aprotic solvents AcN/DMAc by about 15% as given in the method section. This leads to further destabilization of the anionic solute redox state down-shifting the redox potentials correspondingly. Thus, yielding good agreement between computed and measured E^0_{redox} values as is evident form Table 3.11 and Figure 3.15.

Table 3.17. The computed solvation energies $\Delta\Delta G_{solv}$ for the considered compounds are listed in column 2-4 ($\Delta\Delta G_{solv}$ in H_2O) and five 5-7 ($\Delta\Delta G_{solv}$ in AcN and DMAc). DMAc was employed in experiments, which considered the $E°_{redox}$ of the radicals benzoylthiyl and carbthiyl. Solvent dielectric constants, solvent radii and solute atomic radii are used as explained in section 3.2.1 and 3.2.3 and 2.7. All energies are given in eV.

	$\Delta\Delta G_{solv}$ [eV]					
	water			ACN/DACA		
substances	**G3MP2**	**B3LYP**	**B3LYP-S**	**G3MP2**	**B3LYP**	**B3LYP-S**
phenoxyl radical						
4-NO2-Ph-O$^{\bullet}$/O^{-}	–2.365	–2.369	–2.369	–2.039	–2.039	–2.039
4-H-Ph-O$^{\bullet}$/O^{-}*	–2.980	–2.997	–2.997	–2.577	–2.573	–2.573
4-Cl-Ph-O$^{\bullet}$/O^{-}*	–2.711	–2.687	–2.687	–2.347	–2.326	–2.326
4-CH_3-Ph-O$^{\bullet}$/O^{-}*	–2.885	–2.869	–2.869	–2.507	–2.494	–2.494
4-CHO_3-Ph-O$^{\bullet}$/O^{-}	–2.843	–2.873	–2.873	–2.452	–2.480	–2.480
4-NH_2-Ph-O$^{\bullet}$/O^{-}	–2.749	–2.720	–2.720	–2.348	–2.325	–2.325
p-benzoquinone						
O=Ph=O/O=Ph-O$^{\bullet-}$	–2.623	–2.618	–2.618	–2.246	–2.246	–2.246
phenylthiyl radical						
4-NO2-Ph-S$^{\bullet}$/S^{-}	–2.092	–2.095	–2.232	–1.865	–1.861	–1.997
4-H-Ph-S$^{\bullet}$/S^{-}*	–2.684	–2.644	–2.855	–2.382	–2.351	–2.560
4-Cl-Ph-S$^{\bullet}$/S^{-}	–2.428	–2.445	–2.633	–2.158	–2.170	–2.360
4-CH_3-Ph-S$^{\bullet}$/S^{-}	–2.601	–2.602	–2.809	–2.317	–2.307	–2.505
4-CHO_3-Ph-S$^{\bullet}$/S^{-}	–2.590	–2.595	–2.807	–2.317	–2.290	–2.491
4-NH_2-Ph-S$^{\bullet}$/S^{-}	–2.631	–2.668	–2.867	–2.346	–2.300	–2.512
p-benzodithiyl						
S=Ph=S/S=Ph-S$^{\bullet-}$	–2.221	–2.258	–2.347	–1.967	–1.942	–2.133
benzoyloxyl radical:						
Ph-COO$^{\bullet}$/O^{-}*	–2.975	–2.946	–2.946	–2.528	–2.511	–2.511
CH3-Ph-COO$^{\bullet}$/O^{-}	–2.970	–2.919	–2.919	–2.500	–2.489	–2.489
carboxyl radical						
C2H5-COO$^{\bullet}$/O^{-}*	–3.254	–3.213	–3.213	–2.741	–2.728	–2.728
benzoylthiyl radical:						
Ph-COS$^{\bullet}$/S^{-}	–2.601	–2.598	–2.750	–2.281	–2.279	–2.429
CH3-Ph-COS$^{\bullet}$/S^{-}	–2.588	–2.578	–2.734	–2.311	–2.262	–2.418
CH3O-Ph-COS$^{\bullet}$/S^{-}	–2.543	–2.591	–2.746	–2.259	–2.268	–2.427
carbthiyl radical						
C2H5-COS$^{\bullet}$/S^{-}	–2.796	–2.788	–2.974	–2.448	–2.450	–2.640

Table 3.18. Calculated solvation energies obtained with the vdW radii of solvation given in chapter 2.7 for the listed compounds. While conserving the vdW radii used for water I changed the dielectric constant from 80.0 (water) to 37.0 (ACN/DMAc) and the solvent probe radius (spr).

substances	$\Delta\Delta G_{solv}$ (kcal/mol)		
	ε = 80.0 spr = 1.4	**ε = 37.0 spr = 2.0**	**ε = 37.0 spr = 2.8**
phenoxyl radical			
4-NO2-Ph-$O^{\bullet}/O^{-}$	–2.365	–2.322	–2.311
4-H-Ph-$O^{\bullet}/O^{-}$	–2.980	–2.913	–2.891
4-Cl-Ph-$O^{\bullet}/O^{-}$	–2.711	–2.651	–2.640
4-CH_3-Ph-$O^{\bullet}/O^{-}$	–2.885	–2.820	–2.801
4-CHO_3-Ph-$O^{\bullet}/O^{-}$	–2.843	–2.800	–2.753
4-NH_2-Ph-$O^{\bullet}/O^{-}$	–2.749	–2.685	–2.663
p-benzoquinone			
O=Ph=O/O=Ph-$O^{\bullet-}$	–2.623	–2.571	–2.556
phenylthiyl radical			
4-H-Ph-$S^{\bullet}/S^{-}$	–2.684	–2.632	–2.622
benzoyloxyl radical:			
Ph-$COO^{\bullet}/O^{-}$	–2.975	–2.915	–2.898
benzoylthiyl radical:			
Ph-$COS^{\bullet}/S^{-}$	–2.601	–2.545	–2.534

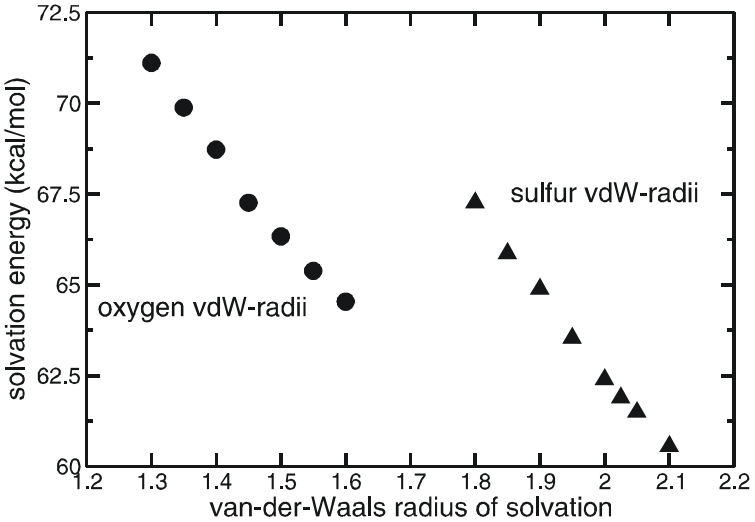

Figure 3.19 Illustration of the dependence of $\Delta\Delta G_{solv}$ in water on the oxygen and the sulfur van-der-Waals radius of solvation. The open circles illustrate $\Delta\Delta G_{solv}$ values for the p-phenoxyl radical with an oxygen radius varied between 1.3 Å and 1.6 Å. The triangle documents the dependence of $\Delta\Delta G_{solv}$ for the p-thiophenoxyl radical on the sulfur radius, which was varied between 1.8 Å and 2.1 Å.

3.3 Coupled proton and electron transfer reactions

Suitable thermodynamic cycles guided us to obtain accurate pK_a values (see section 3.1.1) and one-electron reduction potentials in the condensed phase (see section 3.2.1) for a broad range of organic molecules. In the first application ΔG_{gas} was evaluated with the QC method DFT (B3LYP[76, 77] or Becke($^1/_2$)[75]) combined with the quadruple ζ basis set cc-pVQZ. Independently of the protonation state only closed shell electronic structures appeared in these applications. It was shown in chapter 3.2 that the DFT functional B3LYP using the augmented cc-pVTZ basis set[79, 80] yielded poor EA values compared to results obtained from a G3MP2[78] computation. Inspection of the quinone reduction cascade (see scheme 3.1) reveals the concomitant occurrence of proton and electron transfer. Hence, a single protocol to calculate pK_a values and one-electron reduction potentials from first principles is mandatory to estimate the energetics of the reduction cascade of quinones. Therefore, I tested the performance of the QC method G3MP2 to reproduce accurately the pK_a values for six molecules, which represent the six chemical groups considered in chapter 3.1.

3.3.1 Estimation of PA and pK_a values with G3MP2

PA values. To analyze G3MP2 I first compared for six compounds (butyric acid, benzoic acid, phenol, glutarimide, pyridine and imidazole) experimental PA values with computed data. Table 3.19 proofs that PA values based on G3MP2 match the corresponding experimental value with high accuracy. The RMS deviation for five of the six compounds considered here amounts to 0.415 kcal/mol. B3LYP/cc-pVQZ yields an RMS deviation of 1.62 kcal/mol and Becke($^1/_2$)/cc-pVQZ of 1.83 kcal/mol. The good agreement of computed PA values based on G3MP2 is illustrated in Figure 3.20. Notice that G3MP2 reproduces the PA values of substances with a titratable O-atom and a titratable N-atom equally well, whereas B3LYP matches only PA values of compounds with a titratable O-atom and Becke($^1/_2$) only PA values of compounds with a titratable N-atom. These results proof that the QC method G3MP2 is most suitable to compute pK_a values.

Table 3.19. Comparison of calculated proton affinities (PA) using the QC method G3MP2 B3LYP/cc-pvqz and Becke($^1/_2$)/cc-pVQZ to experimental PA[a] for three compounds with a titratable O-atom and three compounds with a titratable N-atom

substances	formula	measured	G3MP2	B3LYP	Becke($^1/_2$)
butyric acid	C_3H_7-COOH/COO^-	347.26[a]	346.50	347.97	345.03
benzoic acid	Ph-COOH/$PhCOO^-$	340.76[b]	340.72	341.81	338.95
phenol	Ph-OH/Ph-O^-	350.06[c]	349.91	350.43	347.70
glutarimide	C_5H_4ONHO/ON^-O	----	350.06	351.30	349.48
pyridine	$C_5H_5NH^+/C_5H_5N$	222.28[d]	222.27	224.78	220.88
imidazole	$C_3H_3N_2H_2^+/N_2H$	225.33[d]	225.84	227.57	224.33

[a] Reference 136 [b] Reference 137 [c] Reference 138 [d] Reference 135

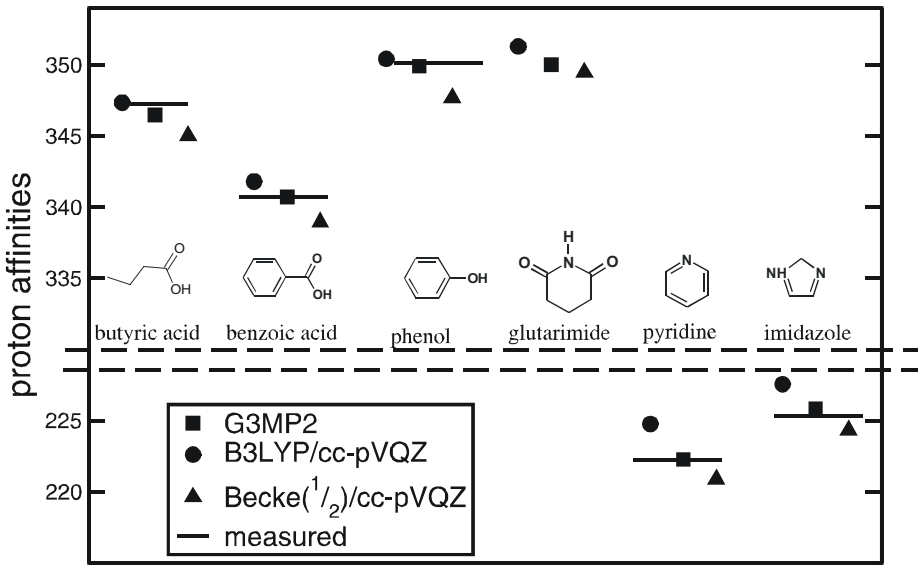

Figure 3.20. Computed PA values obtained with G3MP2, B3LYP/cc-pVQZ and Becke(1/2)/cc-pVQZ are compared with experimental data (dashed line). Figure 3.19 illustrates the accuracy of the G3MP2 method to reproduce PA values accurately for one member of the six functional groups shown in Figure3.1a,b. No experimental value was found in the literature for glutarimide.

pK_a values. Based on computed G3MP2[78] PA values I computed the pK_a values for the above selection of compounds. Table 3.20 reveals that based on G3MP2 excellent agreement with measured data is obtained. The RMS deviation between computed and measured pK_a values is equal to 0.32 pK_a units when G3MP2 is applied. When I compare these results to pK_a values computed with B3LYP[76, 77] or Becke($^1/_2$)[75] we see that G3MP2 is the method of choice. For the six compounds listed in Table 3.20 B3LYP yields an RMS deviation of 0.55 pK_a units and Becke($^1/_2$) of 0.56 pK_a units. In application 3.1, $\Delta G_{solv}(H^+)$ was chosen to minimize the RMS deviation between computed and experimental pK_a values. Based on Becke($^1/_2$) the employed proton solvation of –261.74 kcal/mol was close to the value proposed by Noyes,[84] whereas B3LYP yielded a $\Delta G_{solv}(H^+)$ of –265.94 kcal/mol. With G3MP2 a $\Delta G_{solv}(H^+)$ value = –264.00 kcal/mol , which is close to the latest experiment by Tissandier et al[85] was used. This value has the advantage that it is consistent with the NHE potential of 4.43 eV, which is uniformly used in the scientific literature. If one converts the chemical potential $\mu_{redox} = \mu(H^+/H_2)$ determined from the NHE by Reiss and Heller in 1985[90] into a proton solvation it yields to a $\Delta G_{solv}(H^+)$ = –263.15 kcal/mol (see section 2.7).

Table 3.20. Comparison of calculated pK_a values using the QC method G3MP2 to experimental pK_a values for three compounds with a titratable O-atom and three compounds with a titratable N-atom.

substances	formula	measured	G3MP2	B3LYP	Becke($^1/_2$)
butyric acid	C_3H_7-COOH/COO^-	4.82[a]	4.68	4.93	5.02
benzoic acid	Ph-COOH/$PhCOO^-$	4.22[a]	3.91	3.49	3.26
phenol	Ph-OH/Ph-O^-	9.98[b]	10.31	9.95	9.99
glutarimide	C_5H_4ONHO/ON^-O	11.75[c]	11.61	11.58	12.29
pyridine	$C_5H_5NH^+/C_5H_5N$	5.26[d]	5.31	5.82	5.26
imidazole	$C_3H_3N_2H_2^+/N_2H$	7.00[e]	7.58	7.98	7.82

[a] Reference 3 [b] Reference 40 [c] Calculated using Advanced ChemistryDevelopment (ACD) Software Solaris V4.67 (1994–2003,ACD) [d] Reference 159 [e] Reference 164

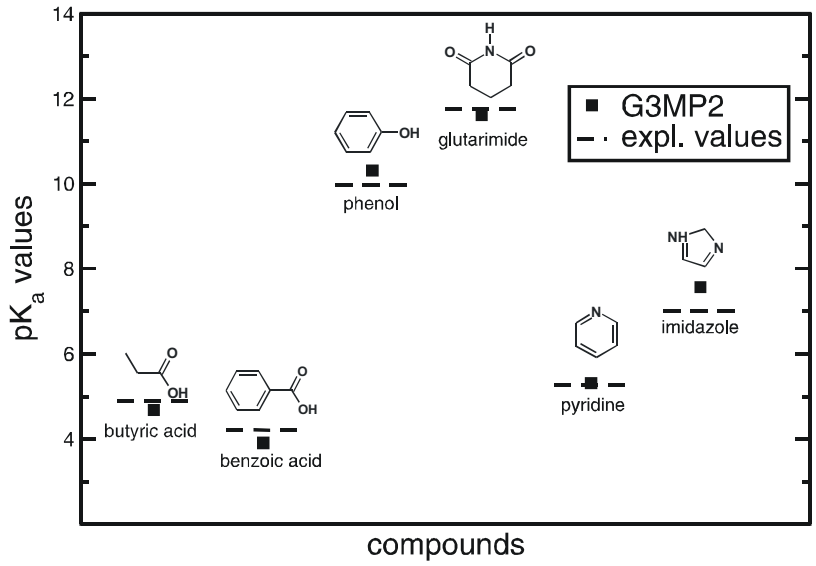

Figure 3.21. Comparison of experimental (dashed line) and calculated (closed squares) pK_a values for six compounds, which represent the six functional groups depicted in Figure 3.1a,b. The considered compounds are depicted in their neutral state. The computed pK_a values are based on electronic energies E_0 obtained with G3MP2, atomic partial charges derived from a QC computation with B3LYP/6-31G** and a $\Delta G_{solv}(H^+)$ value of –264.00 kcal/mol.

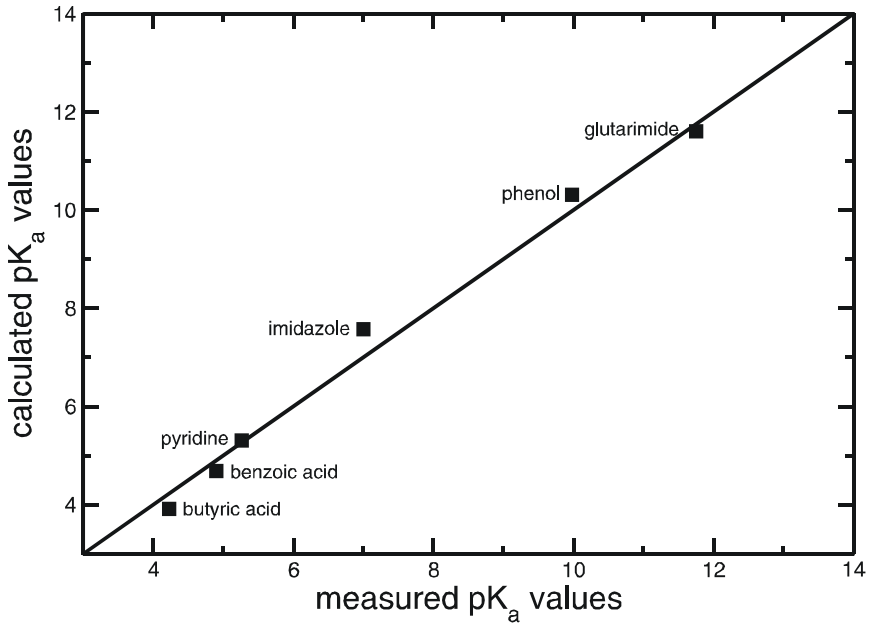

Figure 3.22. Correlation diagram of experimental and calculated pK_a values of six titratable groups depicted in Figure 3.1a,b. Optimized geometries, electronic and vibrational energies in the gas phase were computed with G3MP2 implemented in GAUSSIAN03.[131] Solvation energies were calculated using atomic partial charges obtained with B3LYP/6-31G** and with a $\Delta G_{solv}(H^+)$ value of –264.00 kcal/mol.

3.3.2 Modeling the reduction cascade of p-benzoquinone

Inspection of Table 3.21 reveals that the computed and measured redox-potentials match exactly for the first electron uptake.[27, 28] The computed E^0_{redox} value of the double-electron double-proton uptake underestimates the experimental redox potential by only 0.067 V.[159] Regarding the experimental uncertainty of 0.040-0.050 V this can be considered as a good agreement. This means that we have obtained agreement with those experimental data that can be considered as reliable. The computed E^0_{redox} values of the second electron uptake (Q^- / Q^{2-}) and the double electron uptake (Q / Q^{2-}) are 0.081 V and 0.174 V,[160] respectively lower than the experimental results (see Table 3.21.). In aqueous solution the double negative hydroquinone is immediately protonated yielding QH^-. The polarographic waves of Q^{2-} and QH^- are indistinguishable for experimentalists.[160] Therefore the E^0_{redox} which refer to the Q^{2-} have be taken with caution. It seems that our computed quinone redox potentials, which are not subject to disturbing side should be taken into account.

Taking into account the experimental uncertainty, because of multiple side reactions computed pK_a values match with experimental data. Regarding the RMS deviation of our method the computed pK_a value for the deprotonation from QH to Q^- is in the range of five. This computed value is supported by the observation that quinones are protonated by weak acids as benzoic acid or acetic acid. pK_a values of the QH_2 and QH^- are deduced from spectroscopic data. As mentioned, QH^- is subject for many reactions, which hampers the accurate evaluation of the two

pK_a values. Our computed values exceed the measured values of QH_2 and QH^- by 1.40 and 2.40, respectively.

Scheme 3.1: The reduction cascade of p-benzoquinone to semiquinone and hydroquinone as it occurs in protic solvents through a double electron and proton uptake is illustrated.

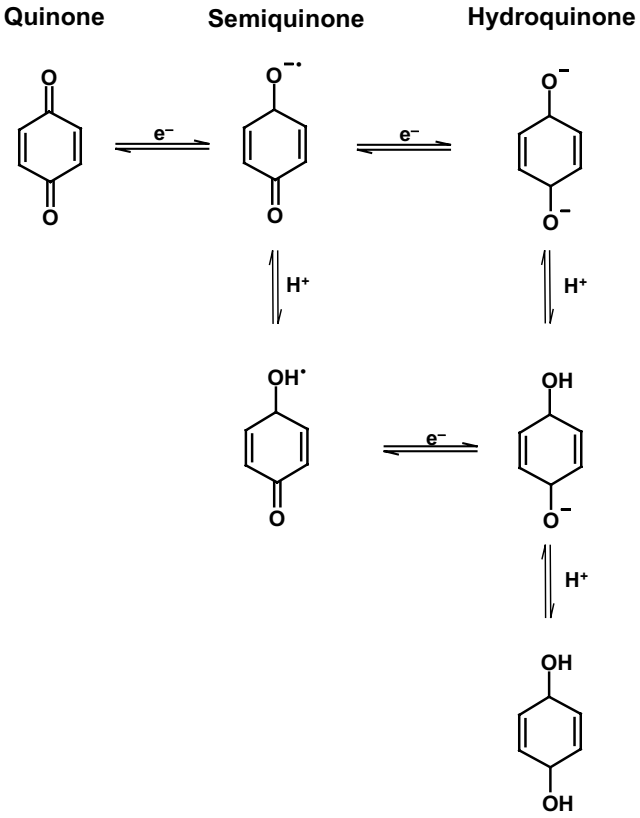

Table 3.21. Comparison of computed and calculated data using the QC method G3MP2 and the *two-step* procedure to compute free electrostatic solvation energies, which is explained in section 3.1 and 3.2 and 2.7 in detail.

1,4-benzoquinone		**G3MP2**	**measured**	**deviation**
reaction:	**type:**	**eV**	**eV**	**eV**
$Q + e^- \rightarrow Q^{-\bullet}$	$E°_{redox}$	+0.110	+0.105[a]	0.005
$Q + 2e^- \rightarrow Q^{2-}$	$E°_{redox}$	+0.205	+0.286[b]	0.081
$Q^{-\bullet} + e^- \rightarrow Q^{2-}$	$E°_{redox}$	+0.299	+0.473[b]	0.174
$QH^{\bullet} + e^- \rightarrow QH^-$	$E°_{redox}$	+0.480	– – – –	– – – –
$Q + 2H^+ + 2e^- \rightarrow QH_2$	$E°_{redox}$	+0.633	+0.699[c]	0.066
$QH + \rightarrow Q^{-\bullet} + H^+$	pK_a	5.10	≅ 4.1 – 4.9[b]	≅ 1.0 – 0.2
$QH^- + \rightarrow Q^{2-} + H^+$	pK_a	13.80	≅ 11.90[d]	≅ 1.90
$QH_2 \rightarrow QH^- + H^+$	pK_a	10.80	≅ 9.90 – 10.00[d]	≅ 0.85

[a] Reference 27,39 [b] Reference 160 [c] Reference 159 [d] Reference 11,12